2016-06

Development of energy absorption structures based on carbon nanofiber foams and shear thickening fluids

Dominguez, Charliean

Monterey, California: Naval Postgraduate School

NAVAL POSTGRADUATE SCHOOL

MONTEREY, CALIFORNIA

THESIS

DEVELOPMENT OF ENERGY ABSORPTION STRUCTURES BASED ON CARBON NANOFIBER FOAMS AND SHEAR THICKENING FLUIDS

by

Charliean Dominguez

June 2016

Thesis Advisor: Claudia Luhrs
Second Reader: Garth Hobson

Approved for public release; distribution is unlimited

THIS PAGE INTENTIONALLY LEFT BLANK

REPORT DOCUMENTATION PAGE			*Form Approved OMB No. 0704–0188*

1. AGENCY USE ONLY *(Leave blank)*	**2. REPORT DATE** June 2016	**3. REPORT TYPE AND DATES COVERED** Master's Thesis

4. TITLE AND SUBTITLE DEVELOPMENT OF ENERGY ABSORPTION STRUCTURES BASED ON CARBON NANOFIBER FOAMS AND SHEAR THICKENING FLUIDS	**5. FUNDING NUMBERS**
6. AUTHOR(S) Charliean Dominguez	
7. PERFORMING ORGANIZATION NAME(S) AND ADDRESS(ES) Naval Postgraduate School Monterey, CA 93943-5000	**8. PERFORMING ORGANIZATION REPORT NUMBER**
9. SPONSORING /MONITORING AGENCY NAME(S) AND ADDRESS(ES) N/A	**10. SPONSORING/MONITORING AGENCY REPORT NUMBER**

11. SUPPLEMENTARY NOTES The views expressed in this thesis are those of the author and do not reflect the official policy or position of the Department of Defense or the U.S. Government. IRB Protocol number ____N/A____.

12a. DISTRIBUTION/AVAILABILITY STATEMENT Approved for public release; distribution is unlimited	**12b. DISTRIBUTION CODE**

13. ABSTRACT (maximum 200 words)

The objective of this thesis was to engineer multifunctional nanostructures, based on carbon nanofiber foams (CNFF), to improve their energy absorption. To attain the goal, experimental research was conducted that combined the CNFF with a) commercial carbon frameworks and b) silica nanoparticles or fumed silica, dispersed on ethylene glycol, forming shear-thickening fluids (STF). The latter were used to fabricate core-shell structures in which the CNFF-STF served as a core and epoxy resin was used as the shell.

The individual nanofibers were characterized by scanning electron microscopy (SEM) and energy dispersive spectroscopy (EDS) methods while the STF rheology was examined as a function of the strain rate. The mechanical properties of the CNFF-STF specimens and the core-shell composites were determined through cyclic compression and hardness measurements/impact tests, respectively.

It was found that the CNFF/commercial frameworks combination generated structures that were too brittle for the desired application. However, the combination of CNFF-STF encased by an epoxy layer resulted in core-shell structures with significant improvements in energy absorption, up to 140% higher when compared to bare epoxy and 33% better when compared to CNFF/epoxy.

14. SUBJECT TERMS Carbon nanofiber foam fabrication, shear thickening fluids, rheology, strengthening, energy absorption, mechanical testing and characterization methods.	**15. NUMBER OF PAGES** 77
	16. PRICE CODE

17. SECURITY CLASSIFICATION OF REPORT	**18. SECURITY CLASSIFICATION OF THIS PAGE**	**19. SECURITY CLASSIFICATION OF ABSTRACT**	**20. LIMITATION OF ABSTRACT**
Unclassified	Unclassified	Unclassified	UU

NSN 7540–01-280-5500 Standard Form 298 (Rev. 2–89) Prescribed by ANSI Std. 239–18

THIS PAGE INTENTIONALLY LEFT BLANK

Approved for public release; distribution is unlimited

DEVELOPMENT OF ENERGY ABSORPTION STRUCTURES BASED ON CARBON NANOFIBER FOAMS AND SHEAR THICKENING FLUIDS

Charliean Dominguez
Lieutenant, United States Navy
B.S., United States Naval Academy, 2010

Submitted in partial fulfillment of the
requirements for the degree of

MASTER OF SCIENCE IN MECHANICAL ENGINEERING

from the

NAVAL POSTGRADUATE SCHOOL
June 2016

Approved by: Claudia Luhrs
Thesis Advisor

Garth Hobson
Second Reader

Garth Hobson
Chair, Department of Mechanical and Aerospace Engineering

THIS PAGE INTENTIONALLY LEFT BLANK

ABSTRACT

The objective of this thesis was to engineer multifunctional nanostructures, based on carbon nanofiber foams (CNFF), to improve their energy absorption. To attain the goal, experimental research was conducted that combined the CNFF with a) commercial carbon frameworks and b) silica nanoparticles or fumed silica, dispersed on ethylene glycol, forming shear-thickening fluids (STF). The latter were used to fabricate core-shell structures in which the CNFF-STF served as a core and epoxy resin was used as the shell.

The individual nanofibers were characterized by scanning electron microscopy (SEM) and energy dispersive spectroscopy (EDS) methods while the STF rheology was examined as a function of the strain rate. The mechanical properties of the CNFF-STF specimens and the core-shell composites were determined through cyclic compression and hardness measurements/impact tests, respectively.

It was found that the CNFF/commercial frameworks combination generated structures that were too brittle for the desired application. However, the combination of CNFF-STF encased by an epoxy layer resulted in core-shell structures with significant improvements in energy absorption, up to 140% higher when compared to bare epoxy and 33% better when compared to CNFF/epoxy.

THIS PAGE INTENTIONALLY LEFT BLANK

TABLE OF CONTENTS

LIST OF FIGURES

THIS PAGE INTENTIONALLY LEFT BLANK

LIST OF TABLES

THIS PAGE INTENTIONALLY LEFT BLANK

LIST OF ACRONYMS AND ABBREVIATIONS

µm	micrometer
ACS	American Chemical Society
ASME	American Society for Testing and Materials
BSE	Back Scatter Electron
C_2H_4	Ethylene
cm	Centimeter
CNT	Carbon Nanotube
CNFF	Carbon nanofiber foam
CoFFiN	Constrained Formation of Fibrous Nanostructures
EDS	Energy Dispersive Spectroscopy
H_2O_2	Hydrogen Peroxide
HCl	Hydrochloric Acid
IF-WS_2	Inorganic fullerene tungsten disulfide
MJ	Mega Joules
MPa	Mega Pascal
N	Newtons
NPS	Naval Postgraduate School
N_2	Nitrogen
mm	Millimeter
nm	Nanometer
O_2	Oxygen
Pd	Palladium
PPE	Personal Protective Equipment
PPI	Pores per Inch
S	Sulfur
SCCM	Standard Cubic Centimeters per Minute
SE	Secondary Electron
SEI	Secondary Electron Image
SEM	Scanning Electron Microscope
SiO_2	Silica

STF	Shear Thickening Fluid
UHP	Ultra High Purity
WS_2	Tungsten Disulfide

ACKNOWLEDGMENTS

First and foremost I would like to give thanks to God for giving me the opportunity to attend the Naval Postgraduate School (NPS) and strength to accomplish my thesis. I would also like to thank the following people for the arduous hours spent in collaboration of my thesis research: Dr. Hugo Zea, Dr. Sarath Menon, and Dr. Chanman Park; Melody Sanchez and Jose Gomez, interns from Hartnell College; and Pedro Arias and Joaquin Tirano, interns from National University of Colombia.

Finally, I would like to thank my thesis advisor, Dr. Claudia Luhrs, for all of her guidance, mentorship, and motivation throughout this experience and in helping me to complete my thesis. Her optimism and confidence in my abilities opened the doors to many unique academic opportunities. I am truly grateful to have had the fortunate opportunity to work under her leadership and for the chance to learn from her expansive knowledge throughout my two years in NPS.

THIS PAGE INTENTIONALLY LEFT BLANK

I. INTRODUCTION

Existing personal protection equipment, from vests, to helmets and boots, among others, consist of diverse materials that offer protection to the wearer but also exhibit shortcomings such as a) they add approximately thirty additional pounds to the wearer, b) its rigidity make it very uncomfortable and c) makes mobility very difficult. Additionally, the current personal protective gear offers very little shock absorption to the user. If there was a material that was lighter, more flexible, and able to absorb the shock of an impact, this could potentially replace the current designs. Through the years, diverse materials have been used, evolving from metals and ceramic combinations to the currently used fabrics (Kevlar, Ultra High Molecular Weight Polyethylene and other aramid fibers) [1-10]. Despite recent advances in the field, further optimization, to not only prevent the piercing of a penetrator but to dissipate the shock of an impact, is needed. In general, improved energy absorption structures are in high demand to protect the lives and well-being of the personnel involved in wide range of activities.

A. PREVIOUS NPS EFFORTS

In order to develop other materials capable of addressing the short comings that the current protective material exhibits, our research team proposed, in previous research, the development, characterization and evaluation of a carbon nanofiber foam (CNFF) as an alternative material. The growth of the three dimensional carbon nanofiber foam was achieved through the constrained formation of fibrous nanostructures process (CoFFiN). The CoFFiN process required for the exact balance of the stoichiometric gas flows of 1:1:6.7 Ethylene (C_2H_4): Oxygen (O_2): Nitrogen (N_2), 10 hour growth time, and 550°C temperature with palladium (Pd) as a catalyst to produce a carbon nanofiber foam. The research conducted at NPS successfully generated a material that was purely inorganic, composed of interwoven carbon nanofiber structure, that has very low density and is mechanically robust, shown in Figure 1. Carbon nanofiber foams have other significant properties, such as high thermal stability of up to 550^{o}C, hydrophobic properties, electrically conductive, present viscoelastic behavior and chemically stable [11-23].

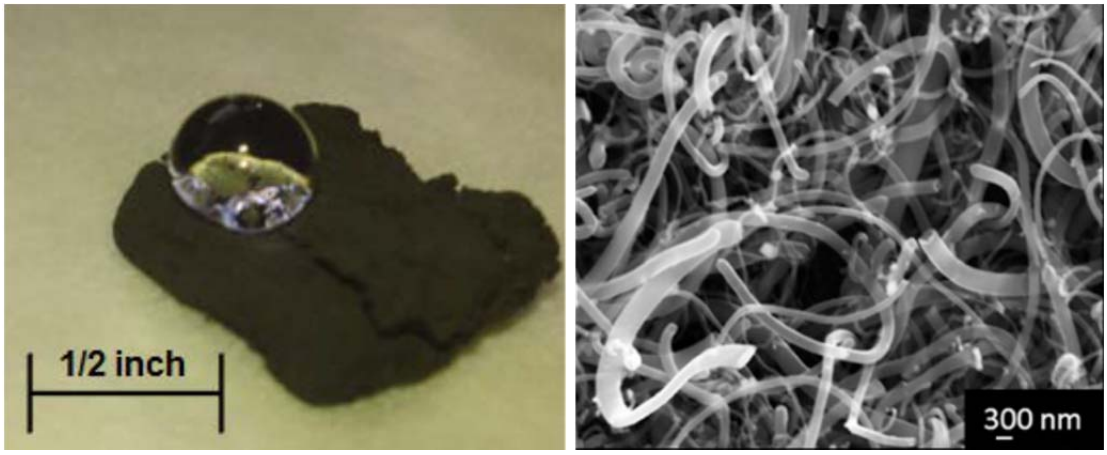

Figure 1. NPS Carbon Nanofiber Foam. Source: [19]

B. THESIS OUTLINE

The main objective of this thesis was to engineer multifunctional nanostructures with improved energy absorption, based on carbon nanofiber foams. In order to achieve this goal, experimental research was conducted that combined the produced carbon nanofiber foam with:

a. Inorganic fullerene tungsten disulfide (IF-WS_2)**,**

b. Carbon frameworks,

c. Shear thickening fluids (STF),

Finally, the best performing hybrid, CNFF/STF was encased in epoxy shell and the mechanical properties of the composite tested.

The rational to use each material was:

a. Inorganic fullerene tungsten disulfide structures are highly resistant to shock and are known for their onion layered microstructures as observed in Figure 2 [24-27]. Including them in a CNFF matrix will also reduce the overall weight of the hybrid structure.

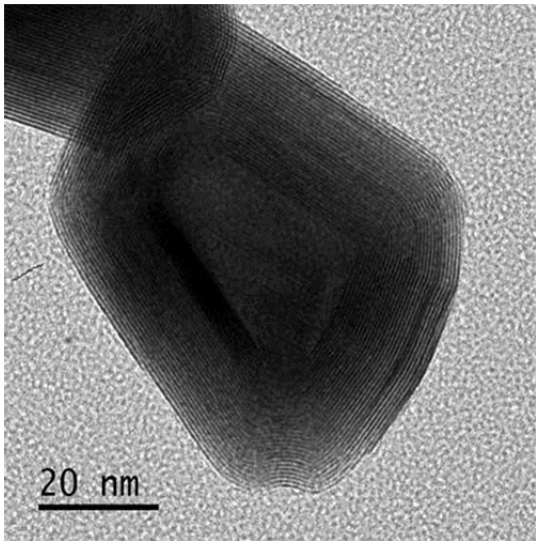

Figure 2. Inorganic Fullerene Tungsten Disulfide Scanning Electron Microscope (SEM) Image

b. Carbon frameworks are known to be brittle, vitreous, highly porous and permeable structures that have low density and high strength to weight ratio as shown in Figure 3. These frameworks provide low fluid resistance, high tolerance of heat and are highly conductive. Carbon frameworks are relatively inexpensive to fabricate at about \$0.09/cm^3 (\$1.50/in^3) and their porous matrix microstructure can be repeated for larger scale applications [28]. The intent to combine the frameworks with CNFF was to provide a backbone structure that could bring additional mechanical stability while keeping its viscoelasticity.

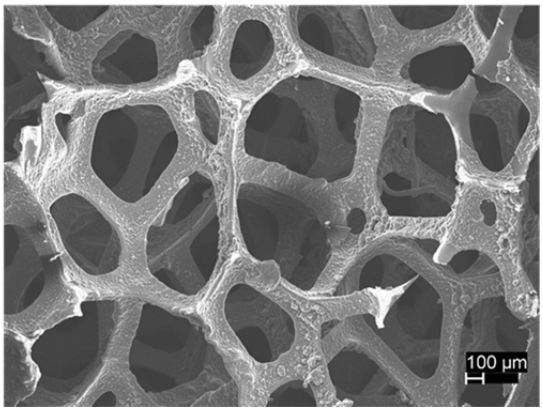

Figure 3. Vitreous Carbon Foam Framework SEM Image

c. Shear thickening fluids consist of a colloidal suspension of particles in a liquid. They are known for their rheological properties; at equilibrium, a shear thickening fluid will behave as a Newtonian fluid but as the shear rate increases they become more viscous and exhibit the behavior and characteristics of a solid, as observed in Figure 4. The shear thickening effect is a reversible process and a shear thickening fluid will return to its fluid state once the shear rate is returned to its equilibrium. Shear thickening fluids may add the strength and stiffness to the CNFF based protective equipment when required and allow for the flexibility and mobility when not [29-32].

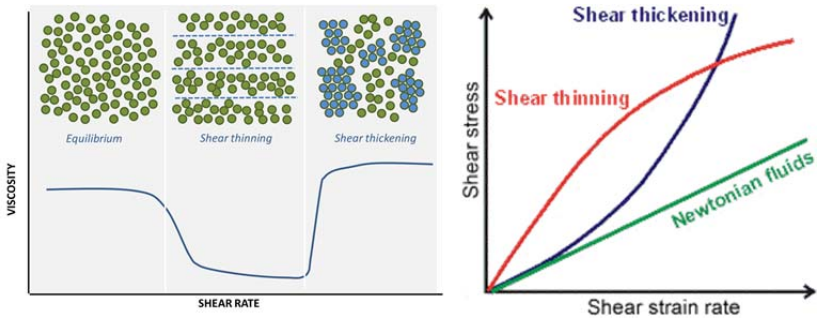

Figure 4. Shear Strain Rate Effects on Viscosity and Stress for Shear Thinning, Shear Thickening and Newtonian Fluids

The combination of a CNFF and a STF encased in an epoxy shell structure designed to contain the STF, given that at low strain rates the later behaves as a fluid and could easily escape the structure. The strategy to use CNFF and STF core-shell epoxy structures required for a viscoelastic material to be at the core surrounded by a STF encased inside an epoxy shell, as depicted in Figure 5.

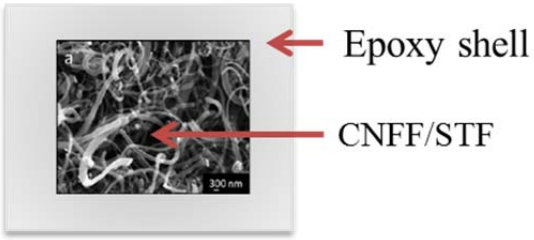

Figure 5. CNFF and STF Core-Shell Epoxy Structures

In order to remove some of the road blocks that could be found when trying to scale up the use of this material, extra effort was undertaken to remove the expensive catalyst (palladium) used during the carbon nanofiber growth.

The results of this research could greatly contribute to the understanding and material selection of personal protection applications. This documented research is separated into six chapters that include an introduction, experimental methods, characterization techniques, mechanical testing, results, discussion and conclusion. The first chapter introduces the need for improved personal protective equipment, types of material traditionally used and motivation for the formulations we proposed. The second chapter describes in detail the experimental processes of all samples observed in this study. The third chapter focuses on the characterization techniques used to obtained additional information of the individual generated samples. The fourth chapter explains the methods and conditions for the mechanical tests conducted on all the specimens. The fifth chapter reveals the results, analysis and discussion of all the collected data from the mechanical testing and characterization methods. The six chapters is the final chapter for this research development and includes summary of all the accomplished work and future research recommendations.

C. THESIS OBJECTIVES

The main goal of this thesis was to provide procedures and experimental approaches to produce materials that could contribute to the improvement of energy absorbing properties of personal protective equipment. In particular, we aimed to:

1. Analyze the viscoelastic properties of carbon nanofiber foams and compare them to commercially available foams.

2. Fabricate and characterized the microstructure and mechanical properties of carbon nanofiber foams that incorporate a) inorganic fullerene tungsten disulfide nanoparticles, b) carbon frameworks, and c) shear thickening fluids.

3. Manufacture and evaluate the energy absorption of epoxy composites that contain the carbon nanofiber foam in combination with shear thickening fluid.

4. Establish a methodology to remove the palladium catalyst from the carbon nanofiber foam to reduce fabrication cost and open the possibility to scale up production.

D. HYPOTHESES

1. Carbon nanofiber foams have higher energy absorption than commercially available foams used for damping applications.

2. The production of carbon nanofiber foam in combination with inorganic fullerene tungsten disulfide (IF-WS_2) will improve energy absorption properties of the CNFF.

3. Incorporation of the CNFF with carbon frameworks will strengthen the CNFF and increase energy absorption of the foam.

4. The production of carbon nanofiber foam in combination with a shear thickening fluid will improve energy absorption properties of a CNFF and STF epoxy core-shell structure.

5. The removal of the Palladium catalyst from the foam will not significantly alter the mechanical properties of the CNFF.

II. EXPERIMENTAL METHODS

A. OVERVIEW

The experimental methods presented herein include the procedures followed in order to fabricate carbon nanofiber foams, combine the CNFF with IF-WS_2, carbon frameworks and shear thickening fluid formulations. Based on the results for the later, CNFF were used as core and encased in epoxy shells, all with the goal of improving the mechanical properties of the multifunctional structures. For the generation of shear thickening fluids we used two different types of silica particles. The steps taken to produce core-shell structures required the design and manufacture of two molds, which are also outlined in this chapter.

B. GROWTH OF CARBON NANOFIBER SAMPLES

The process for growing carbon nanofiber foam was adopted from previous research based on the constrained formation of fibrous nanostructures (CoFFiN) process [14, 19]. Using the prior work as a starting point, the flows were increased maintaining the stoichiometric balance to optimize the foam quality of the previously grown carbon nanofiber foam.

1. Carbon Nanofiber Foam Synthesis Process

Based on prior research, the growth of carbon nanofiber foam required a combination of a fuel rich mixture of a hydrocarbon and oxygen to react with a catalyst. Ethylene (C_2H_4) gas was the carbon source selected for the foam growth and palladium was used as the catalyst. The process took place at a reaction temperature of 550°C.

A previously designed mold made of 304 stainless steel was used for the use of the carbon nanofiber foam growth. The mold constrained the growth of the foam to the measurements of 11.25 cm in length, 12.5 cm in width and 1.9 cm in thickness. The mold preparation followed the procedures as outlined by prior research [14, 19].

For the CNFF synthesis, 500 milligrams of the palladium powder (Aldrich submicron >99.9%) were measured and placed evenly in a diagonal pattern around the

base of the rectangular mold as shown in Figure 6. A series of gas flow deflectors made of stainless steel shim (Trinity Brand Industries, Inc., Part No. 6316–4) were inserted on top to direct the reactive gases to fill the chamber, followed by the mold cover as shown in Figure 6b. The mold was then sealed with stainless steel socket head cap screws (ASME B18.3), lubricated with anti-seize (Type B Versachem High Temp Copper formula), and each of the screws were torqued to 1.7 Newton meter using a torque wrench.

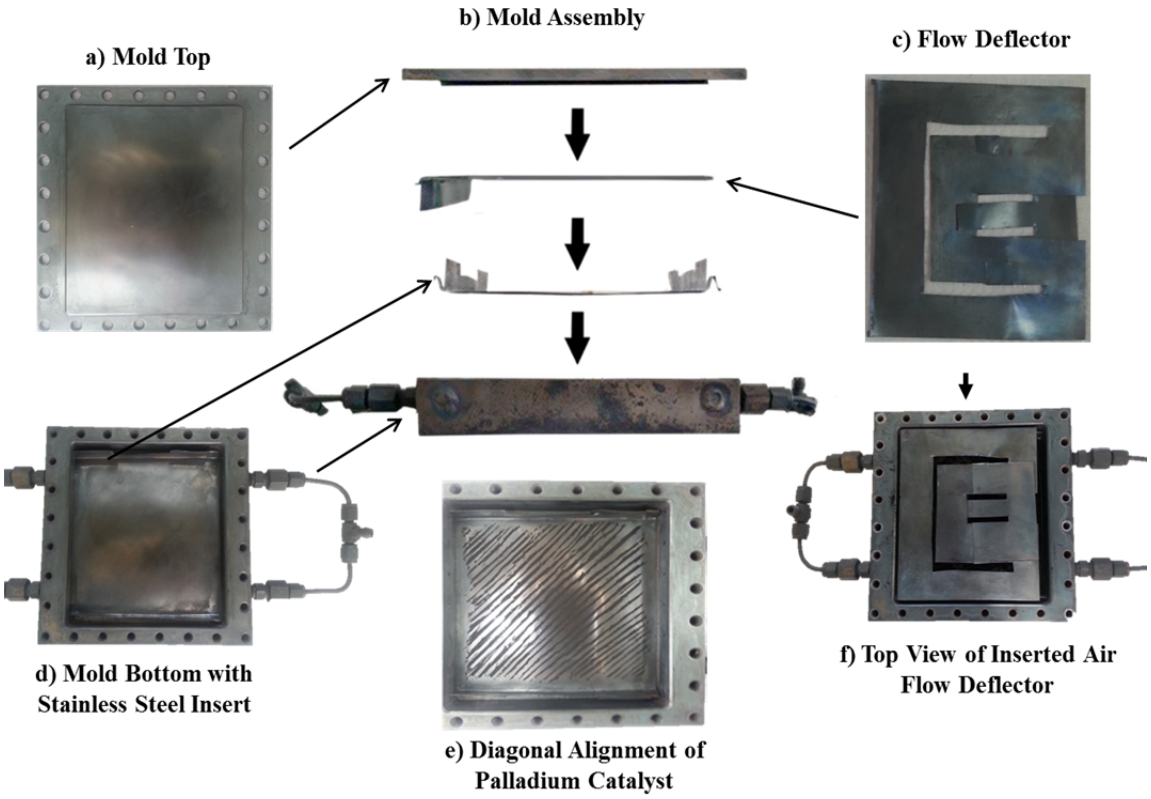

Figure 6. Carbon Nanofiber Foam Mold Assembly

The assembled mold was then attached to the serpentine inlet and outlets and placed inside the furnace. The inlet flow was connected and controlled by the multi gas flow controller model MKS 647. The furnace was heated to the 550°C set point and an initial flow of 300 standard cubic centimeters per minute (SCCM) of nitrogen gas (N_2, Praxair, UN1066, UHP >99.9%) was used for 30 minutes with the intent of removing air

from the system. At the end of 30 minutes, the N_2 flow was increased to 330 SCCM and 50 SCCM of ethylene (C_2H_4) and 5 SCCM of oxygen (O_2). The oxygen flow was increased by 5 SCCM every two minutes until it reached the desired gas flow of 50 SCCM. After five hours, the furnace, the oxygen and the ethylene flows were turned off. The nitrogen flow was reduced to 10 SCCM and the furnace was allowed to cool to room temperature. Figure 7 depicts the various equipment and set ups used in this procedure.

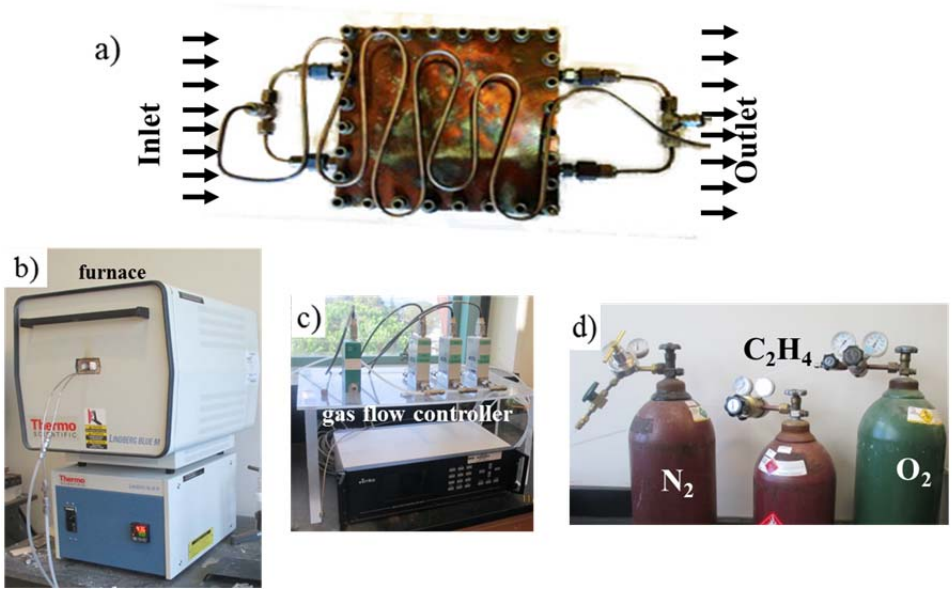

Figure 7. Carbon Nanofiber Foam Synthesis. a) Mold containing catalyst, b) furnace, c) gas flow controller and d) gases employed.

2. Catalyst Recovery Method

As a proof of concept regarding the possibility of reducing the cost for growing carbon nanofiber foams, the palladium catalyst was removed from the foam. The proposed methodology consisted of submerging the CNFF in an acidic aqueous solution of 10% hydrochloric (HCl) acid (Sigma-Aldrich ACS reagent) and 5% Hydrogen Peroxide (H_2O_2) (Sigma Aldrich 30% solution). The solution was then heated and maintained at a temperature of 60°C using a heating plate. The temperature was monitored using a thermal imaging FLIR XI series camera as shown in Figure 8a. Seven

samples of CNF foam were equally cut and six of them were placed into the 50 mL beakers that contained the heated acidic aqueous solution. Samples were removed from the solution as 0, 15, 30, 60, 90, 120 minutes and 18 hrs had elapsed. The samples were then cleaned with distilled water and ethanol and allowed to dry as shown in Figure 8b. SEM analysis was employed to determine if the palladium was successfully removed.

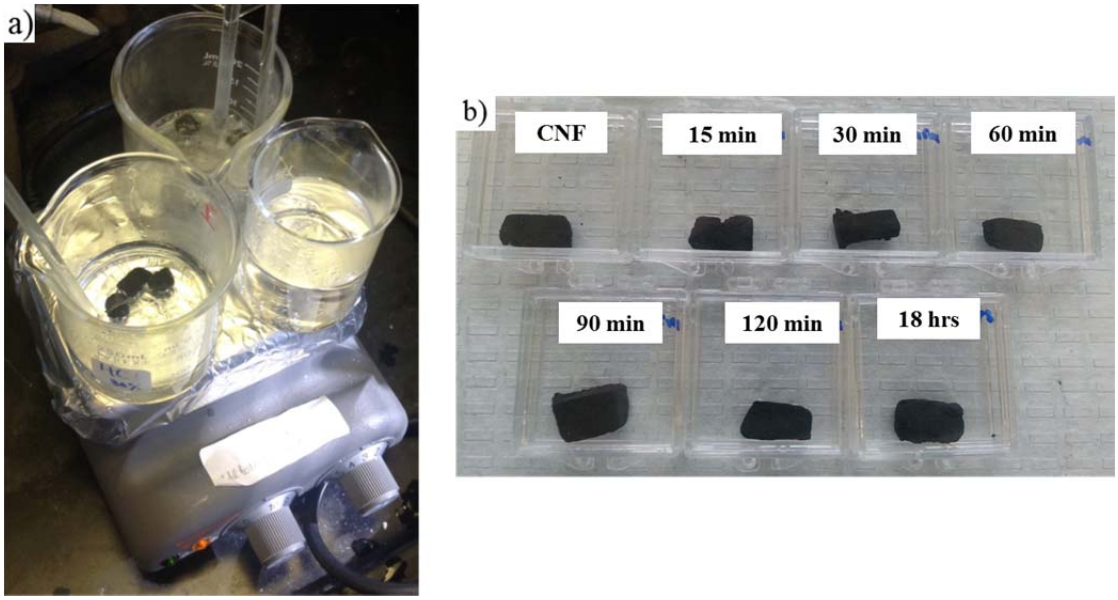

Figure 8. Catalyst Removal Process

C. CARBON NANOFIBER IMPREGNATION WITH FULLERENE TUNGSTEN DISULFIDE

The wet impregnation procedure was used to combine the carbon nanofiber foam with IF-WS_2 to create an even dispersion of IF-WS_2. The process consisted of saturating the CNFF with IF-WS_2 nanoparticles dispersed in ethanol. After impregnation the solvent was evaporated at 60°C allowing for the penetrated tungsten disulfide to remain.

The CNFF was impregnated with 1% and 10% IF-WS_2 by weight. Samples of CNFF were then cut into two cylinder shapes with a diameter of 12.64 mm and thickness of 6.21 mm for mechanical testing.

A heating plate and the ceramic dish shown in Figure 9 were used while impregnating the CNFF up to supersaturation point with the generated IF-WS_2 and

ethanol aqueous solution. The heating plate temperature was monitored using a thermal imaging camera FLIR xi series to allow for the ethanol of the IF-WS_2 and ethanol solution to evaporate from CNFF inside of the ceramic dish and expedite the diffusion process.

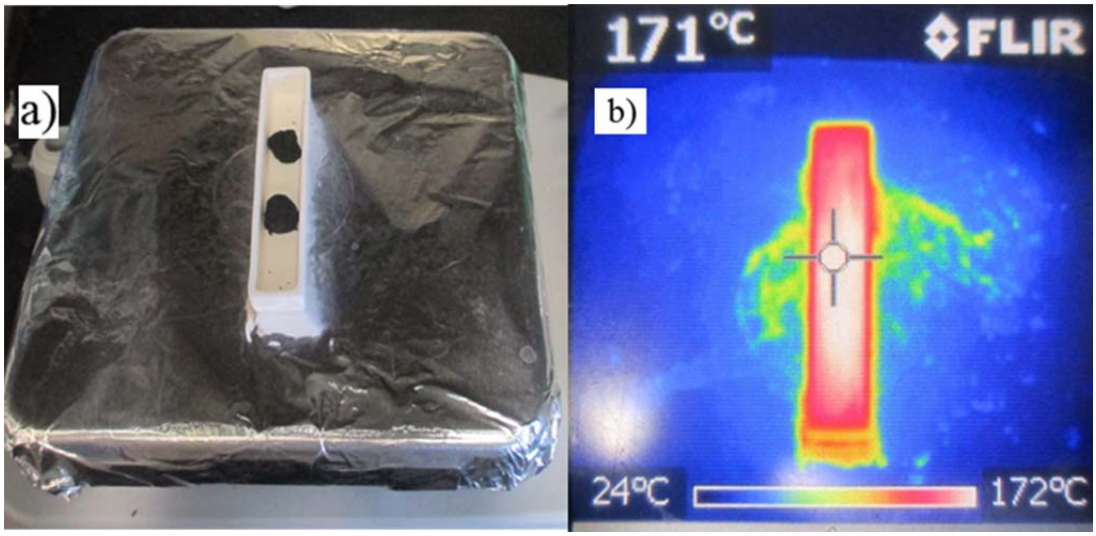

Figure 9. Carbon Nanofiber Foam Impregnation of Tungsten Disulfide Using Heating Plate and Infrared Image Collected from Thermal Imaging Camera FLIR xi Series

D. GROWTH OF CARBON NANOFIBER USING CARBON FRAMEWORKS

Commercially obtained carbon rigid framework foams (Duocel Reticulated Vitreous Carbon Foam, 3% density) with porosity range of 10 through 100 pores per inch (PPI) were used as a backbone in the growth process of the CNFF, some of them shown in Figure 10. The objective was to use the commercial vitreous foams as a framework that the CNFF would grow into and to test the mechanical properties of the resulting hybrid structure. Two different strategies were used:

1. The catalyst was placed below the frameworks.
2. The catalyst was wet impregnated into the framework.

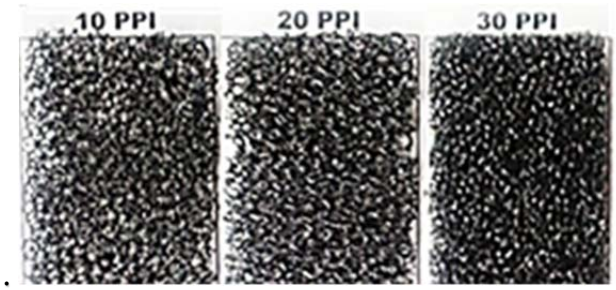

Figure 10. Carbon Commercial Foams with Porosity of 10 PPI, 20 PPI, and 30 PPI

Catalyst on the base. The rectangular pieces were cut to measure between 44.47-45.19 mm in length, 37.02-39.22 mm in width, and 6.99 mm-7.82 mm in thickness. Prior to placing the rectangular pieces of vitreous carbon foam into the inlet flow side of the mold 500 milligrams of the palladium catalyst was evenly distributed throughout the mold in a diagonal patterned as shown in Figure 11.

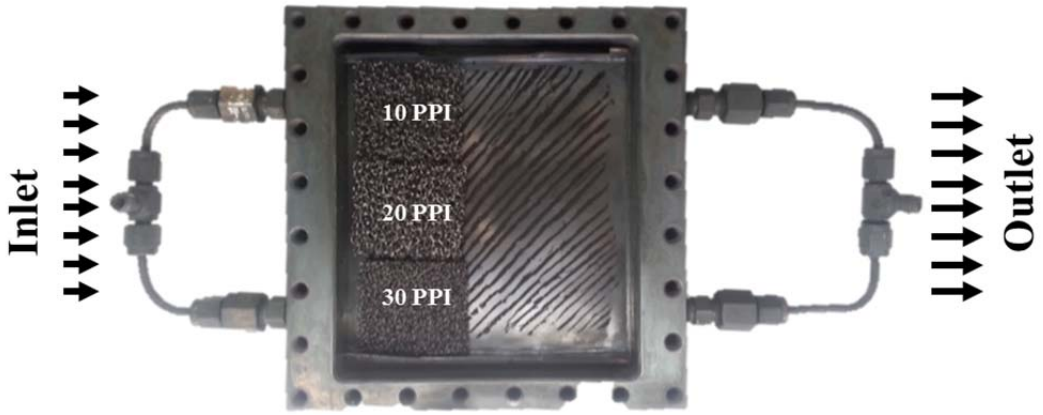

Figure 11. Carbon Nano Fiber Foam Grown Using a Vitreous Carbon Foam Framework.

Impregnated catalyst. The second method included three commercial vitreous carbon foams that were 45, 80, and 100 PPI respectively as shown in Figure 12. The rectangular pieces were cut to measure between 43.89 mm-45.40 mm in length, 38.75-40.67 mm in width, and 6.32 mm-6.59 mm in thickness. A suspension of 500 mg of

palladium in methanol (Sigma Aldrich anhydrous 99.8%) was deposited in the porous structure by wet impregnation as shown in Figure 12.

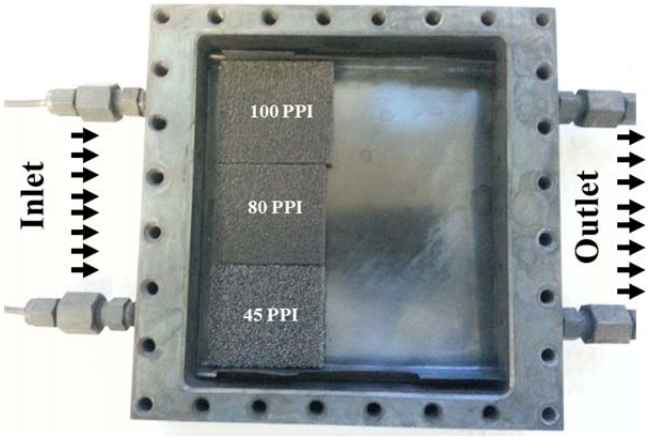

Figure 12. Wet Impregnation of Carbon Nanofiber Foam Grown Using a Vitreous Carbon Foam Framework.

1. Carbon Framework and Carbon Nanofiber Foam Growth

The synthesis process remained the same as the optimize carbon nanofiber process discussed earlier in the chapter for all of the carbon nanofiber grown using the different frameworks.

E. GENERATION OF SHEAR THICKENING FLUID

Two shear thickening fluids were produced using samples of Silica: one of them used SiO_2 nano-powder (Sigma-Aldrich, 5–15 nm, 99.5% trace metals) and the other fumed silica powder (Sigma-Aldrich, .007 µm).

1. Shear Thickening Fluid Generation with Silica Nano Particles

The initial shear thickening fluid samples generated were produced using silicon dioxide nano-powder (Sigma-Aldrich, 5–15 nm (TEM), 99.5% trace metals) in a suspended solution of ethylene glycol (Sigma-Aldrich, 99.8% anhydrous). The silica nanoparticle shear thickening fluids were generated by a colloidal suspension composed of 20%, 30% and 40% of SiO_2 nano-powder by weight in ethylene glycol.

2. Shear Thickening Fluid Generation with Fumed Silica Particles

Subsequently, three additional shear thickening samples were generated using fumed silica powder (Sigma-Aldrich, .007 μm) and ethylene glycol (Sigma-Aldrich, 99.8% anhydrous) suspensions composed of 20%, 30% and 37% of fumed SiO_2 powder by weight in ethylene glycol. Attempts to produce a sample with 40% fumed silica were unsuccessful since the solid would not disperse in ethylene glycol and reached a saturation point at 37% fumed silica powder by weight.

3. Shear Thickening Fluid Generation with Inorganic Fullerene Tungsten Disulfide Nano Particles

Efforts to produce a shear thickening fluid using inorganic fullerene tungsten disulfide (Nano Material) and ethylene glycol (Sigma-Aldrich, 99.8% anhydrous) suspension were tried. However, the particles were too dense to be dispersed even at low concentrations of 10% and 20% of IF-WS_2 by weight in ethylene glycol and no further characterization or testing of this sample was pursued.

F. EPOXY ENCASING OF CARBON NANO FIBER AND COMMERCIAL FOAM SAMPLES

Since one of the main objectives for this research was to determine how much energy was absorbed by the different types of foams and included additives in comparison to the CNFF, samples needed to be prepared for impact testing. Two different variations of epoxy foam encasing mold designs were developed to manufacture standardized samples for IZOD impact testing.

1. Epoxy Samples using Stainless Steel Mold

The first mold designed was a three piece mold made of stainless steel milled using a Hass VF-6 CNC 5-degrees of rotation mill that consisted of six individual sample casings. The three piece mold required a locking device to fix the side plates to the bottom plate as shown in Figure 13.

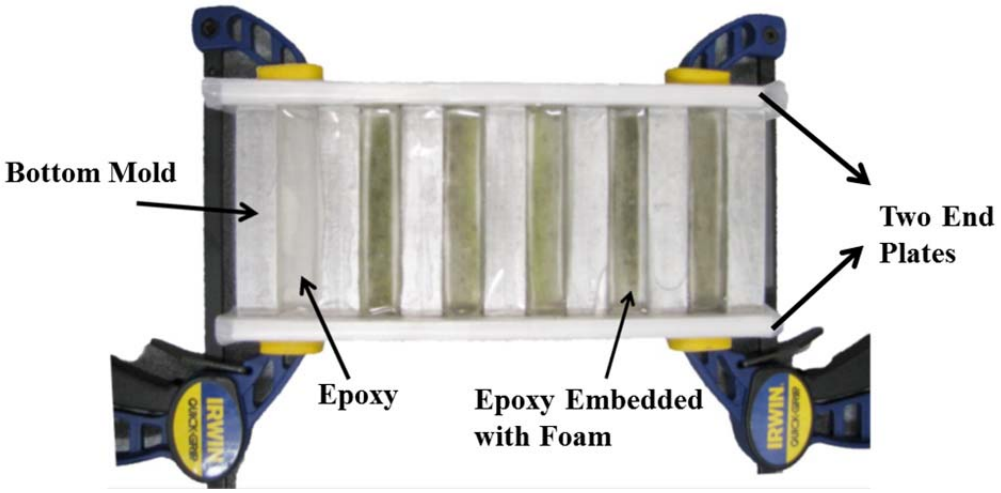

Figure 13. Encasing Process: CNFF/ Commercial Foam Epoxy Samples using Stainless Steel Mold

a. Encasing Process

The epoxy used for all epoxy embedded samples is the Struers Specifix-20 Kit which is a two agent epoxy system that cures at room temperature. The epoxy used for this mold was measured by volume. The ratio of resin to curing agent is 26:5. The steps described in mixing epoxy procedures were followed. Prior to mixing the 26:5 resin to curing agent the mold had to be assembled. The first layer of the epoxy mixture was poured into each of the individual casings by adding the same volume of mixture. This initial layer of epoxy was left to cure at room temperature for twenty four hours. At the end of the curing time the different commercial foams were carefully placed inside the individual casings and then covered by additional resin. This final layer was also left to cure for twenty four hours. After the twenty four hour curing time the side plates were removed and each of the individual epoxy samples were removed from the bottom plate. The foams encased in the initial mold for comparison were the NPS carbon nanofiber foam, the polyethylene foam, and the polyurethane foam as shown in Figure 14. The carbon nanofiber foam used was grown at NPS as described in the carbon nanofiber foam growth chapter.

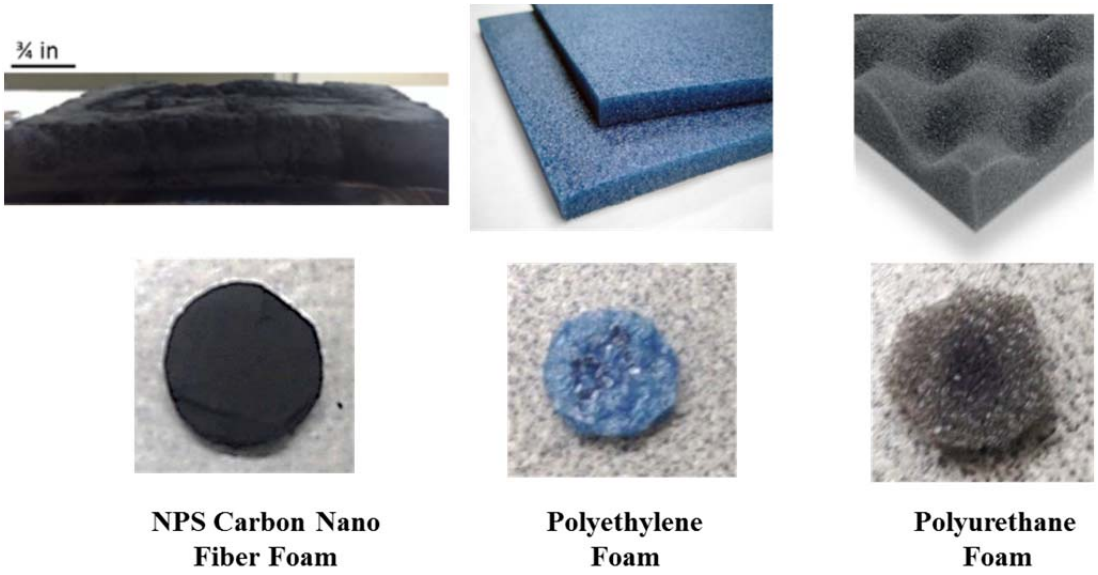

Figure 14. Types of Foam Used for Epoxy Embedded Samples Manufactured with the Stainless Steel Mold. Adapted from [33, 34].

2. Epoxy Samples Using Polymer Mold

The second mold was designed using SolidWorks and manufactured by the Ultimaker 2 Extended three dimensional printer shown in Figure 15 [35].

Figure 15. The Ultimaker 2 Extended Three Dimensional Printer Used to Manufactured the Polymer Mold

The second mold was made out of polymer and consisted of two individual pieces as shown in Figure 16. The bottom mold consisted of eight individually and equally sized sample molds that included the American Society for Testing and Materials (ASTM) standardized notch for IZOD Impact Testing requirements. The ASTM standard measurements are 12.70 mm for width, 63.50 mm for length, and 3.17 mm for thickness per sample. Each of the individual sample molds were designed to also meet these measurement requirements with built in tolerances for the polishing process. The total length of the epoxy mold was 185 mm and width of 80 mm as shown in Figure 16. The top mold consisted of eight smaller extrusions that fit inside the bottom mold casing and would shape the epoxy as it is compress into the bottom mold.

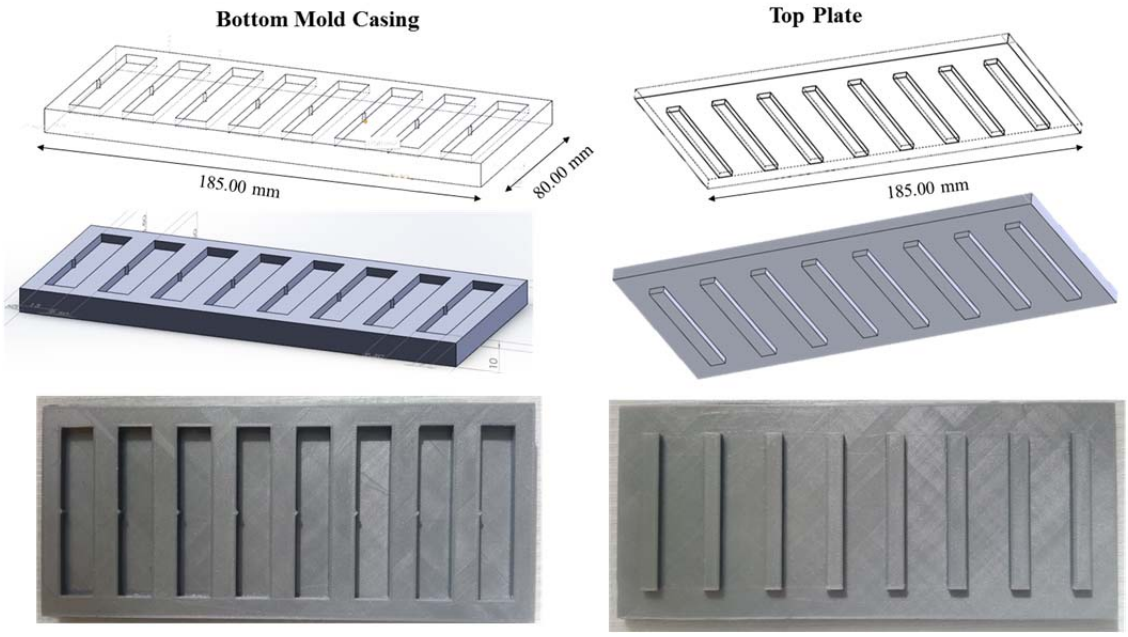

Figure 16. Epoxy Mold II Assembly

a. Epoxy Encasing Process

The epoxy encasing process is a five step process. First the top and bottom of the mold needs to be covered with a very thin film of white petrolatum to prevent the epoxy from becoming permanently attached to the mold. The epoxy used for all epoxy embedded samples is the Struers Specifix-20. Second, 20 g of resin and 3 g of curing

agent were mixed to generate the epoxy. The mixture was then poured into each of the eight spaces until all of them were completely filled as shown in Figure 17.

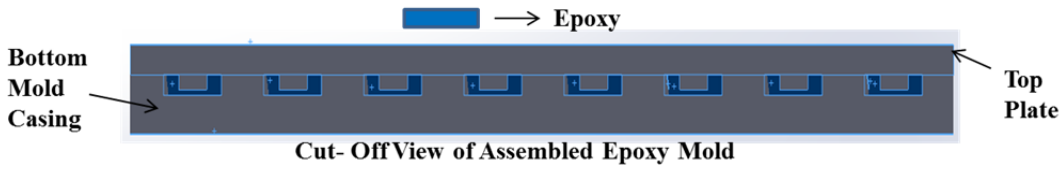

Figure 17. Cut-Off View of Assembled Epoxy Mold

The top of the mold was placed on top of the bottom and compressed with five pound metal weight. Finally, the compressed mold was placed in a -10 mm Hg vacuum for 24 hours to remove any excess air that may have become trapped within the wetted epoxy as shown in Figure 18.

Figure 18. Epoxy Mold Under Vacuum

Upon completion of the 24 hours the top of the mold was removed and eight cured and harden epoxy sample molds were revealed as shown in Figure 19.

Figure 19. Epoxy Mold II with Eight Individually Harden Epoxy Molds.

The eight individual samples were removed from the mold and each sample was filled as shown in Figure 20. The samples containing the shear thickening fluids were placed in a vacuum for an additional hour prior to encapsulating them with the top layer of epoxy. The final samples after the polishing procedures are shown in Figure 20.

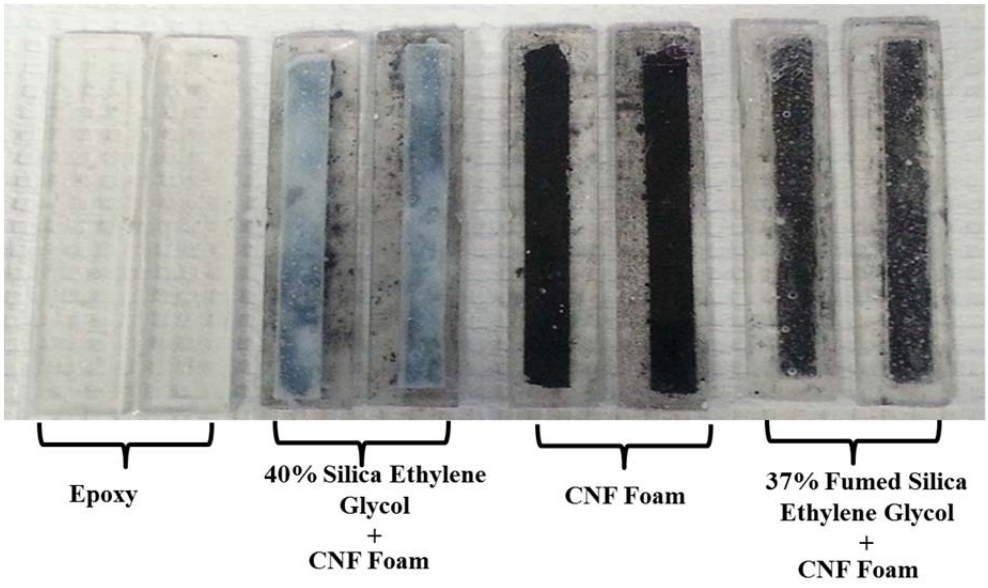

Figure 20. IZOD Impact Tester Epoxy/STF/CNFF Embedded Samples

THIS PAGE INTENTIONALLY LEFT BLANK

III. CHARACTERIZATION TECHNIQUES

A. OVERVIEW

This chapter highlights the characterization methods used to analyze the carbon nanofiber foams microstructure and the different samples that were generated in the experimental chapter. Methods such as scanning electron microscope (SEM), Energy dispersive spectroscopy (EDS), backscatter electron image (BSE), thermo gravimetric analysis (TGA), differential scanning calorimetry (DSC), hardness tester and image j software were utilized to obtained additional microscopic information of all samples. The use of a shear rheometer was also necessary in order to analyze the produced shear thickening fluids.

B. SCANNING ELECTRON MICROSCOPE

The Zeiss Neon 40 high resolution scanning electron microscope was used to collect the high surface resolution and topographical secondary electron images (SEI), backscattered electron (BSE) images, and the energy dispersive spectroscopy (EDS) of the CNFF produce and the different produced samples of CNFF. The samples viewed also included the carbon nanofiber foam impregnated with IF-WS_2, catalyst removal samples, and the generated carbon nanofiber foam using the different frameworks. [36]

Each of the observed samples were fastened on top of an aluminum sample holder via carbon matrix tape as shown in Figure 21. All the samples were placed inside a vacuum chamber for a period of 24 hrs to allow the removal of all possible gasses within the samples. The SEM field emission gun produced the potential energies used to target the samples with. The high tension potential energies used were between the ranges of 2kV and 20 kV for all the samples. The topographic images obtained from the secondary electron (SE) were collected while the SEM was between a power level of 3 to 10 kV for the carbon nanofiber foam samples and magnification range of 20x up to 100,000x. The backscattered electron images were obtained at an SEM power level between 10 and 20 kV with a magnification range of 20x up to 100 Kx. The SEM was used to obtain high surface or topographic resolution images for different samples [36].

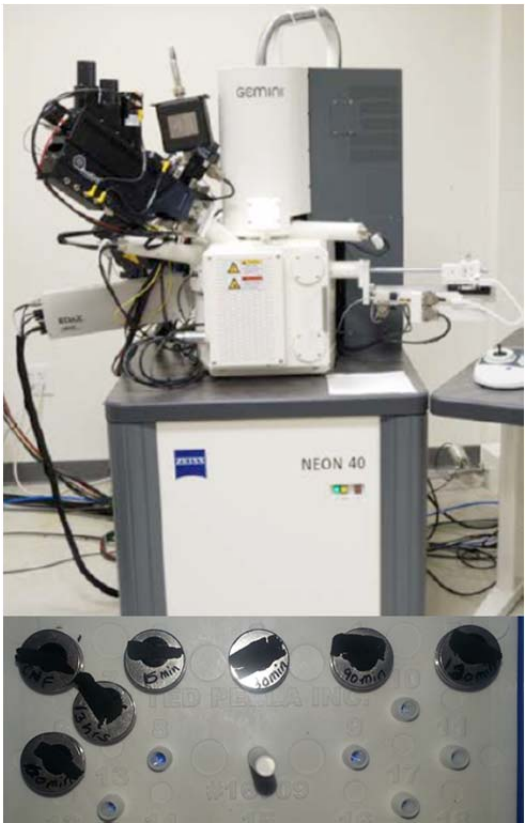

Figure 21. Scanning Electron Microscope and Prepared CNFF Samples

1. Energy Dispersive Spectroscopy

The energy dispersive spectroscopy was used to uses the X-ray spectrum from the electron beam to obtain a chemical analysis of the specimen. EDS enables qualitative and quantitative analysis by identifying the lines in the spectrum and measuring the line intensities for each element in the sample. Element distribution maps can be produced by scanning the electron beam and showing the intensity of a selected X-ray line. The energy dispersive spectroscopy was obtained at an SEM power level of 15 kV, 60µm filter and magnification range of 20x up to 100 Kx.

2. Backscatter Electron Image

The backscatter electron image was used to contrast the palladium particles from the carbon nanofibers in the catalyst removal samples. The backscatter electron images

were obtained at an SEM power level of 10 and 20 kV and magnification range of 20x up to 100 Kx.

C. SHEAR RHEOMETER

The produced shear thickening fluids discussed in the experimental chapter were analyzed for the viscous properties of the fluids using the Bohlin C-VOR Shear Rheometer as shown in Figure 22. The shear rheometer was employed to measure the resulting shear stress that is applied via a cylindrical plate rotating through the shear thickening fluid.

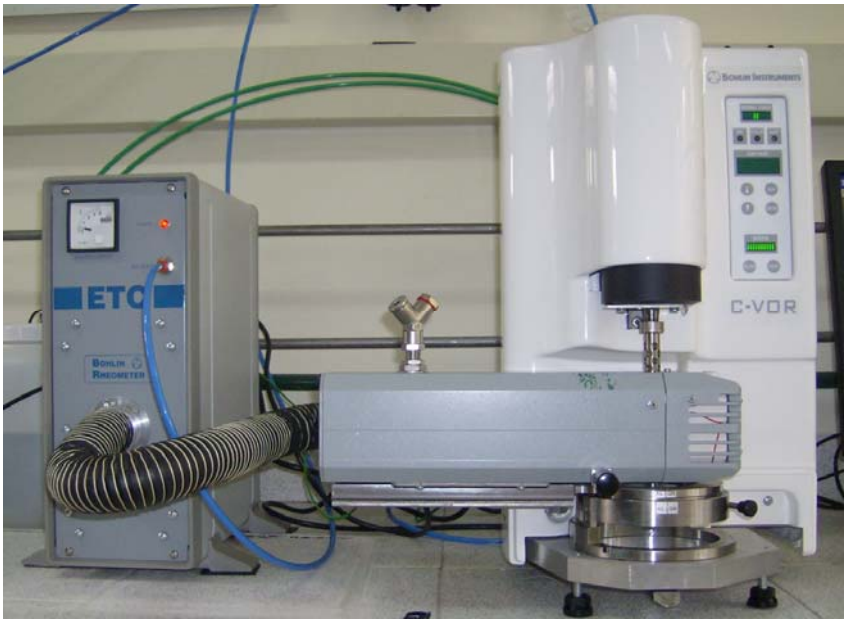

Figure 22. Bohlin C-VOR Shear Rheometer

D. IMAGE J SOFTWARE FOR PARTICLE ANALYSIS

The images collected from the back scattering electron were analyzed using Image J which is an image analyzer computer software. The Image J software was used for particle counting of the produced catalyst removal samples [37] .

THIS PAGE INTENTIONALLY LEFT BLANK

IV. MECHANICAL TEST

A. OVERVIEW

Mechanical testing was conducted for all the fabricated samples discussed in the experimental portion of this research as shown in Table 1. Cyclic testing and compression testing was conducted for the carbon nanofiber foam, commercially obtained foam, and composite foams in a constrained and unconstrained conditions. Compression testing to the point of failure was conducted for all epoxy encased carbon nanofiber foam and commercial foams manufactured by the stainless steel epoxy mold. Impact testing was conducted on all epoxy encased samples. Micro hardness testing was conducted for all epoxy encased CNF foams and commercially obtained foams manufactured by the initial stainless steel epoxy mold.

Table 1. Mechanical Testing Conducted

Mechanical Test	Material	Constrained Cyclic Compression	Unconstrained Cyclic Compression	Unconstrained Compression to Failure	IZOD Impact Test
Foams	CNFF	✓	✓		
	Polyurethane		✓		
	Polyethylene		✓		
Carbon Framework/ CNFF	100 PPI/CNFF			✓	
	80 PPI/CNFF			✓	
Core-Epoxy Shell	Epoxy			✓	✓
	CNFF			✓	✓
	Polyurethane			✓	✓
	Polyethylene			✓	✓
	40% wt SiO_2 STF/ CNFF				✓
	37% wt SiO_2 STF/ CNFF				✓

B. MECHANICAL TESTING OF CARBON NANOFIBER AND COMMERCIAL FOAMS

Cyclic compression testing using an Instron 5942 with a 100 N load cell was conducted for the carbon nanofiber foam and commercially obtained foam in constrained and unconstrained conditions.

1. Constrained Cyclic Compression Mechanical Testing

In order to contain the CNFF samples and preserve the cross sectional area during measurements, a fiberglass mold with an orifice to contain the sample to be measured (13 mm in diameter and 8 mm in height) was employed as shown in Figure 23. The prepared carbon nanofiber foam was mechanically tested under constrained conditions at .03 MPa/sec, .06 MPa/sec and MPa/sec compression rates for the duration of 25 cycles. One cycle is defined by the completion of a complete cycle of loading the sample to 90 N then unloading to 10 N and reloading to 90 N. Each CNFF sample was compressed from an initial force of 0 N to a maximum load of 90 N before the commencement of 25 cycles.

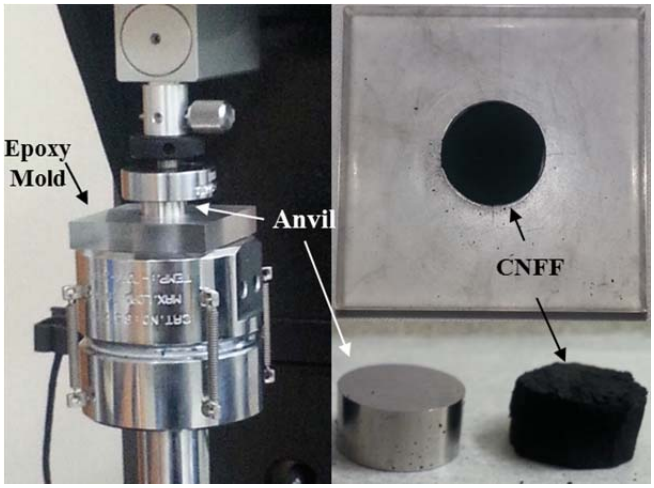

Figure 23. CNFF Cyclic Constrained Mechanical Testing.

2. Unconstrained Cyclic Compression Mechanical Testing

The seven carbon nanofiber samples treated with the acidic aqueous solution for catalyst removal as described in the experimental section of this research were tested

using the Instron 5942 based on unconstrained conditions with a compression rate of .01 mm/ sec for 25 cycles from 10–90 N as shown in Figure 24. The carbon nanofiber foam and commercial foams were tested in similar conditions but using a rate of 0.05 mm/sec.

Figure 24. Carbon Nanofiber Foam Unconstrained Compression Testing

3. Unconstrained Compression Mechanical Testing of Carbon Nano Fiber Foam and Frameworks

The carbon nanofiber foam and carbon frame works with porosities of 45 PPI, 80 PPI and 100 PPI samples were compressed in an unconstrained configuration from 0 N to failure at a compression rate of .01 MPa/ sec. The samples tested measured 10.23 mm-11.94 mm in length, 8.52 mm—9.74 mm in width and 6.08 mm- 6.55 mm in thickness as shown in Figure 25.

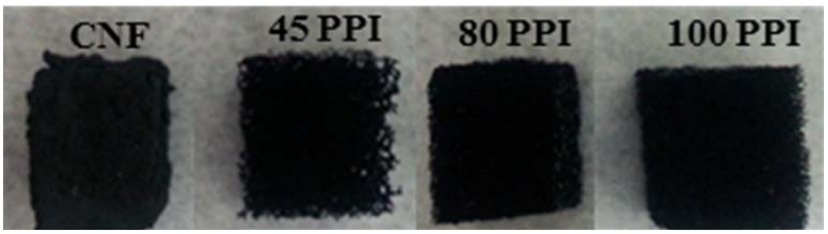

Figure 25. Compression Testing Carbon Nanofiber Foam Framework Samples

C. MECHANICAL TESTING OF EPOXY ENCASED FOAMS

This section will cover the mechanical testing conducted in order to compare the mechanical properties of the carbon nanofiber foam, polyethylene and polyurethane commercial foams encased in an epoxy as shown in Figure 26. All the foams were evaluated by micro hardness, compression, and impact testing.

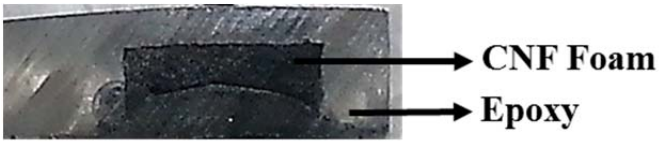

Figure 26. CNFF Encased in Epoxy

1. Hardness Testing

The micro hardness testing on the epoxy embedded samples was performed in a Digital Micro Hardness Tester HVS-1000, shown in Figure 27. Each of the epoxy encased foam samples prepared in the experimental methods were tested in three different locations throughout the sample to test for sample hardness homogeneity and data repeatability.

Figure 27. Digital Micro Hardness Tester HVS-1000

2. Compression Testing

The SATEC Instron extended upgrade (Model MII-20UD) machine with a 200kN cell was used with two flat plates to perform a single compression test. Each of the samples were compressed up to failure at a compression rate of 5 mm/min composite shell. The rectangular epoxy composite pieces were cut to measure between 10.7 mm - 14.2 mm in length, 9 mm-13.58 mm in width, and 5.5 mm- 6.7 mm in thickness.

3. Impact Testing

IZOD impact test was conducted for both the samples manufactured using the initial stainless steel mold with a six sample capacity and the polymer mold with eight sample capacity. The initial mold consisted of the CNFF, commercially obtained foam, and pure epoxy. The secondary mold consisted of the CNFF, CNFF, with the implementation of the two different shear thickening fluids, and pure epoxy.

The IZOD impact test was conducted using the Tinius Olsen model IT504 impact tester in Figure 28. The initial samples obtained by the stainless steel mold did not have a notch per ASTM standard prior to testing. The secondary samples from the polymer mold did have the notch for IZOD impact test as specified by ASTM D256 standard test

method. The impact testing determined the pendulum impact resistance of the specimens and the energy absorbed by the samples in the breaking process.

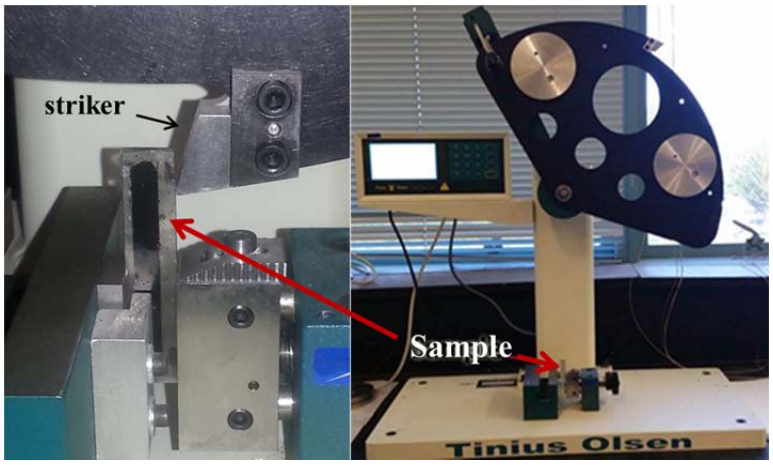

Figure 28. IZOD Impact Test Using the Tinius Olsen Model IT504

V. RESULTS AND DISCUSSION

A. OVERVIEW

This chapter presents and discuss all data generated as a result of performing the experiments described in the three previous chapters. The microstructural analysis of the CNFF growth procedures is described along with the effectiveness of catalyst recovery treatment. The differences between commercial foams and the NPS CNFF are presented and evaluated. The outcome of combining CNFF with IF-WS2 and carbon frameworks are shown. The viscosity of different shear thickening fluids are analyzed and all structures mechanical properties reviewed.

B. CARBON NANO FIBER FOAM

1. Synthesis and Mechanical Properties

The modification of the stoichiometry flows during the CNFF growth process resulted in a foam that filled the mold completely and that was more uniform and structurally robust from previously fabricated foams. The final weight for the grown CNFF was of 24.9713 g as shown in Figure 29.

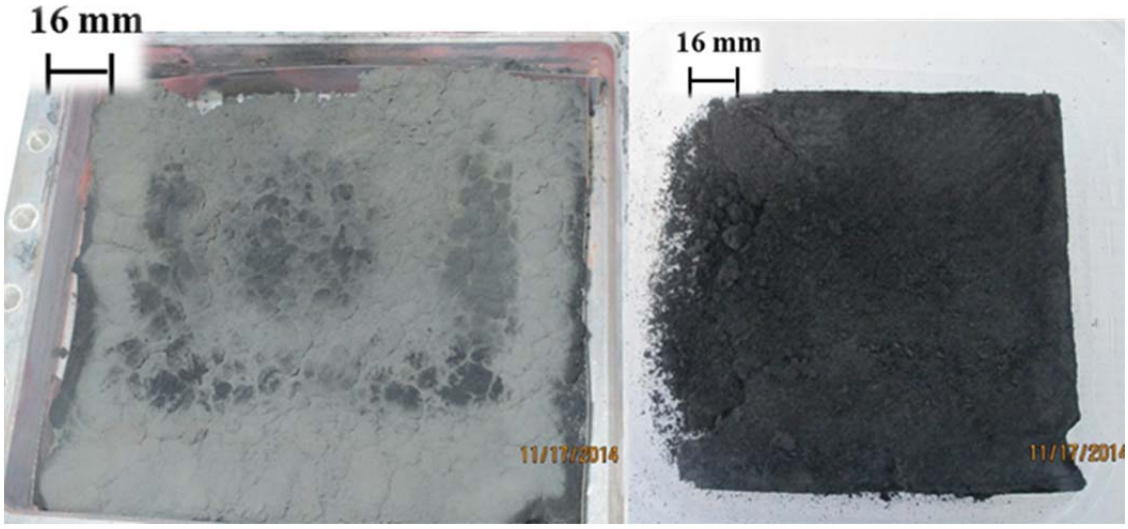

Figure 29. Carbon Nanofiber Foam Gaseous Flow Optimization Results

In order to ensure that the optimized gaseous flows produced the desired carbon nanofiber foam, samples of the grown foam were characterized using the scanning electron microscope. The collected SEM images are shown in Figure 30 and substantiate that the modification of gaseous flows resulted in the growth of intertwined carbon nanofibers of diameter size of 20 nm up to 300 nm which is consistent with previous grown CNFF.

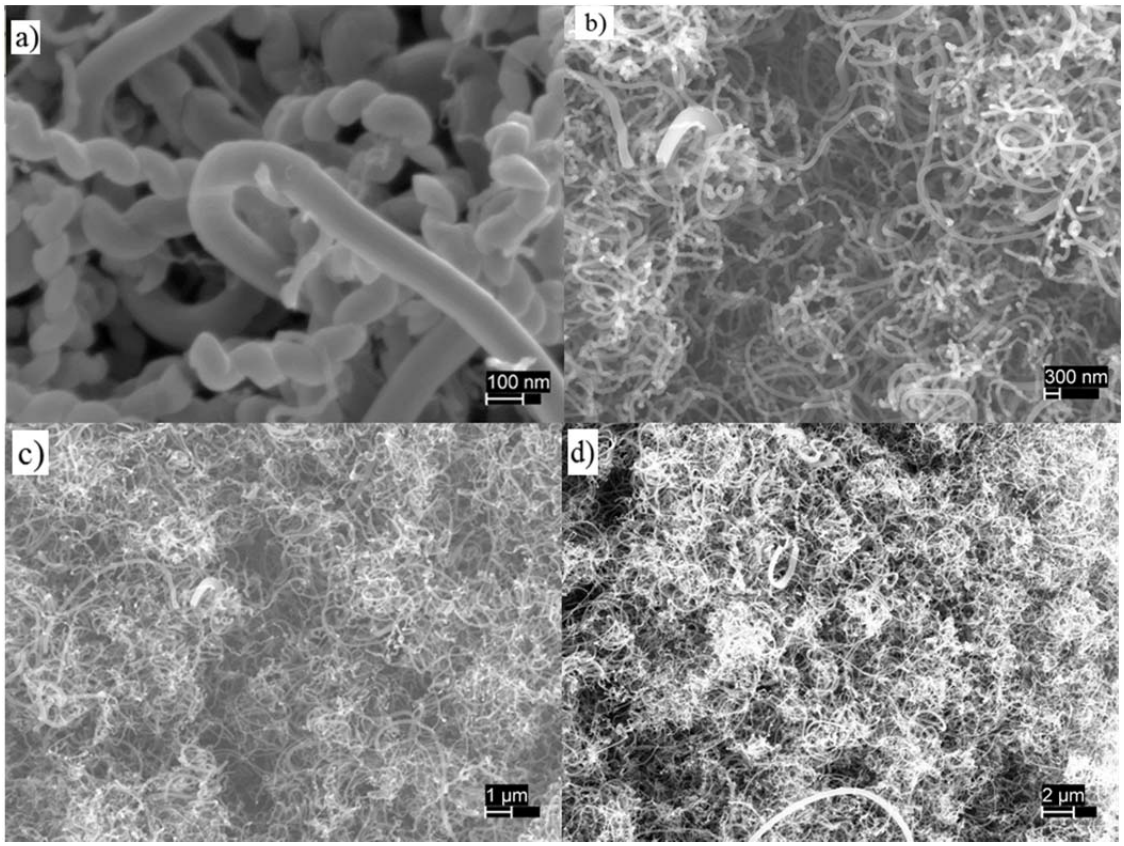

Figure 30. Carbon Nanofiber Foam Scanning Electron Images

The grown carbon nanofiber foam cyclic compression mechanical test, at varied compression rates, exhibited a hysteresis loop as observed in Figure 31. This hysteresis loop is indicative of viscoelastic behavior in the material, which is an expected property of foams. Additionally, as the compression rates are increased the slope of the hysteresis loop at the loading stage increases identifying that the foam is becoming more rigid. The

mechanical performance for the carbon nanofiber foam remains consistent with previously produced carbon nanofiber foams.

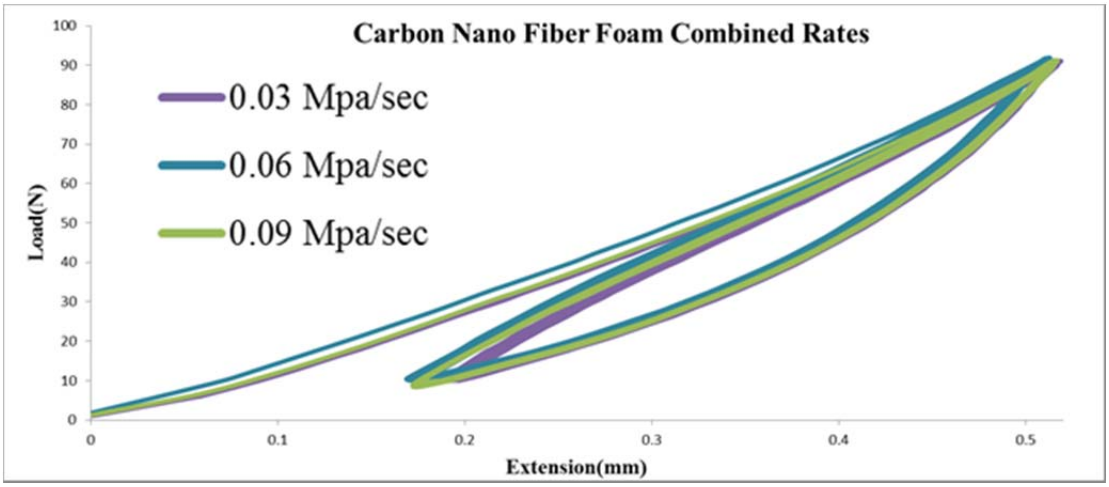

Figure 31. Cyclic Constrained Compression Testing for Carbon Nanofiber Foam Load vs. Extension Results

2. Palladium Removal

In order to reduce manufacturing cost a method for extracting the expensive palladium catalyst was developed in prior research and used for this work as described in the experimental section of this research. The goal was to remove the palladium catalyst without altering the microscopic characteristics and mechanical properties of the grown carbon nanofibers. The results of the performed experiments were examined and validated through the collected SEM images, particle count analysis using image J software, and mechanical testing of the before and after catalyst removal treatment carbon nanofiber foam samples.

In order to collect information as to the impact that the catalyst removal treatment inflicted on the carbon nanofiber foam images were taken using the scanning electron microscope to compare the initial and end conditions of the carbon nanofiber. The images obtained from the carbon nanofiber foam samples using the scanning electron microscopy images were taken at 2 kV and magnification of 75 kX. The carbon nanofiber foam SEM image without catalyst removal treatment is shown in Figure 32a and the

SEM image after the carbon nanofiber sample had been submerged in the catalyst removal acidic treatment for 18 hours is shown in Figure 32b. Comparing the untreated CNFF sample to the treated for 18 hours CNFF sample does not result in degradation of the fibers as observed by the SEM images in Figure 32.

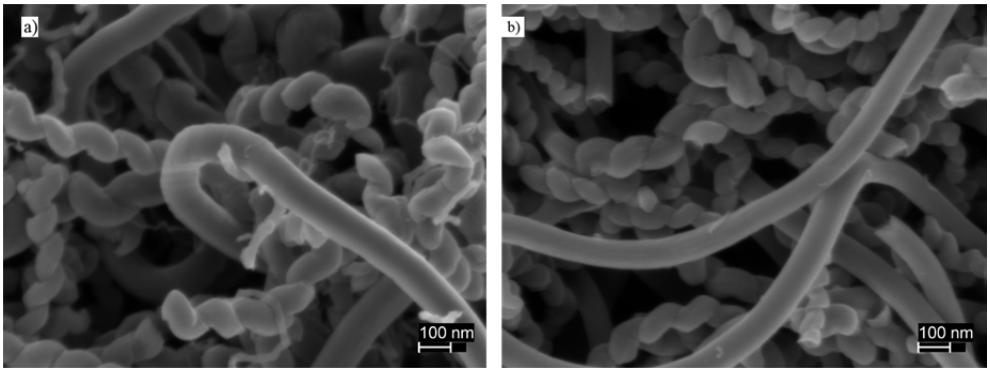

Figure 32. SEM Images of the CNFF: a) Prior to Treatment.
b) After Catalyst Removal Treatment for 18 hours.

The scanning electron microscope was also used to obtain backscattering electron (BSE) images of all the treated samples to evaluate which catalyst removal treatment was the most effective. The collected backscattering images for the untreated, 60 minute, 90 min, and 120 minute catalyst removal treatment are shown in Figure 33. The untreated CNFF sample backscattering image visually exhibit the highest density of palladium as revealed by the bright particles that are contrasted against the dark background as shown in Figure 33a. The catalyst removal treated CNFF sample for 120 min backscattering image visually exhibit the lowest density of palladium as revealed by the lessening of bright particles that are contrasted against the dark background as shown in Figure 33d. The data collected from the BSE images results in the correlation that the time exposed to the catalyst treatment is directly proportional to the amount of extracted palladium from the samples. [14]

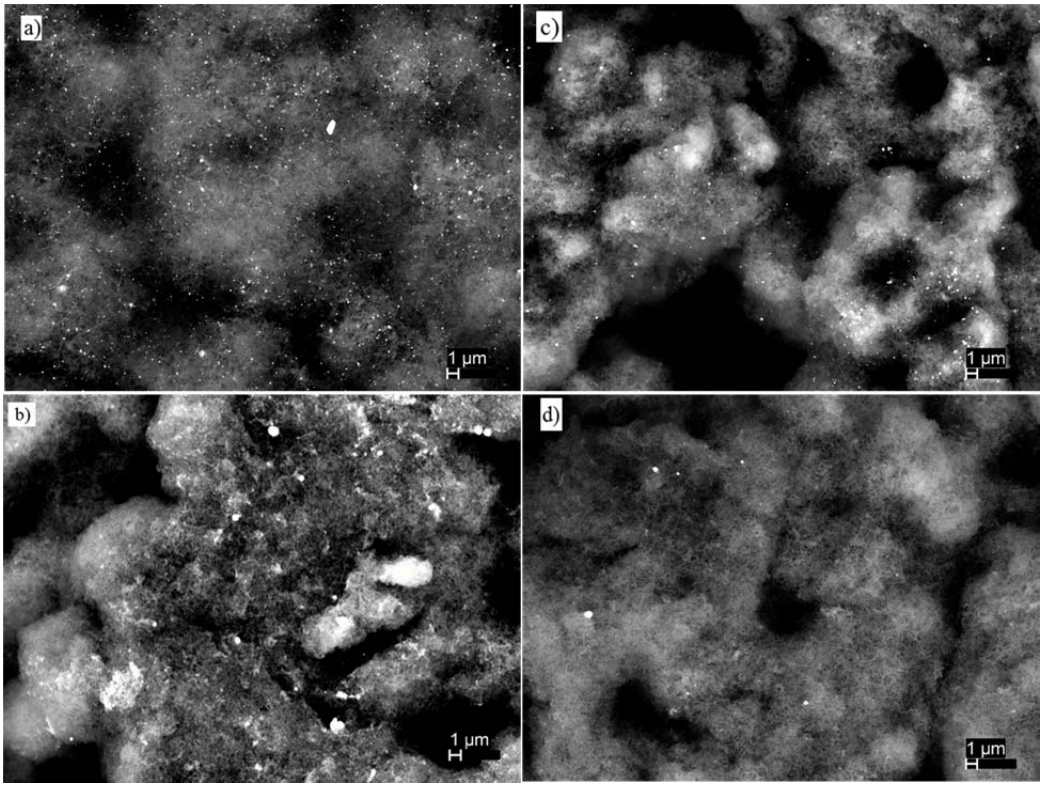

Figure 33. BSE images of a) Untreated CNFF, Catalyst Removal Treated CNFF sample for b) 60 min, c) 90 min, d) 120 min.

In order to verify the effectiveness of the catalyst removal treatment the backscattering images as shown in Figure 34a through Figure 34c of the carbon nanofiber foam treated samples were analyzed using Image J computer software. Image J software converted the obtained backscattering images of the treated samples into binary images based on a given threshold as shown in Figure 34d through 34f. This threshold was set to identify and quantified the black regions represented by palladium particles in each of the produced binary images. Image J based on computational analysis is able to extract the particle count from each of the samples resulting in a palladium to carbon ratio of 1:64 for the untreated carbon nanofiber foam, 1:110 for catalyst removal treatment of 90 minutes and 1: 822 for the catalyst removal treatment of 120 minutes. The image J results exhibits and makes evident the correlation that the longer the carbon nanofiber foam is exposed to the catalyst removal treatment the more palladium particles are extracted from the CNFF. [14]

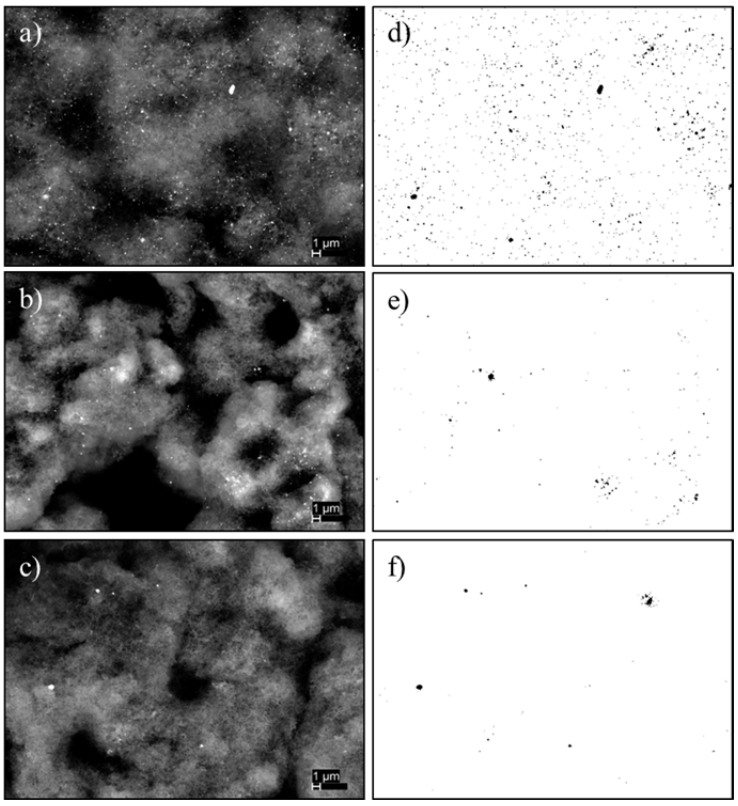

Figure 34. BSE and Image J Analysis of Catalyst Removal Results. a) Untreated CNFF, catalyst removal treatment of b) 90 min, c) 120 min, and d), e) and f) Image J analysis of a), b) and c).

C. CARBON NANO FIBER FOAM VS. COMMERCIAL FOAMS

1. Bare Foams Characterization

The polyethylene foam is a resilient closed-cell chemically cross linked foam which is used to absorb the impact caused by numerous vibration inflicted on a material [34]. The polyurethane foam is an open cell foam that is used as a filter or to provide shock protection [33]. The unconstrained cyclic compression of the carbon nanofiber foam, the polyurethane foam, and the polyethylene foam samples resulted in the behavior expected for a viscoelastic material. The circulation created by the loading and unloading curves from the stress and strain chart as shown in Figure 35 are known as the hysteresis loop. In order to calculate the energy absorbed by each of the different foam the area inside each of the hysteresis loops was calculated. The energy absorption calculations indicated that the carbon nanofiber foam had the highest energy absorption of the tested

foams as shown in Figure 35. The carbon nanofiber foam was able to absorbed almost 95.6% more energy as compared to the polyurethane commercial foam and 77.3% more energy in comparison with the polyethylene commercial foam as shown in Figure 35. Overall, cyclic compression mechanical testing of the polyurethane foam and the polyethylene commercial foam samples demonstrate minimal energy absorption capability in comparison to the CNFF.

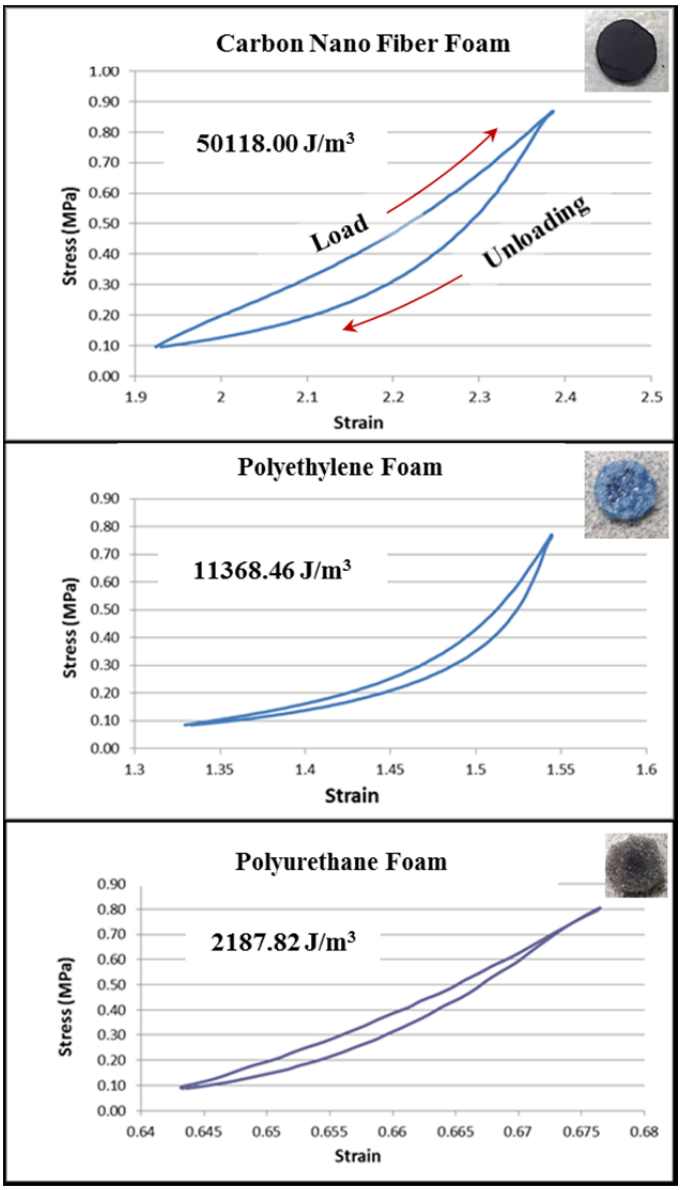

Figure 35. Unconstrained Cyclic Compression Testing of CNFF vs. Commercial Foams

2. Epoxy Shell- Foam Core Characterization

The micro hardness results for all the tested epoxy encased CNFF samples represented only the surface characteristics. This resulted in the values for the micro hardness test to be dominated by the epoxy shell and not the carbon nanofiber foam, polyethylene foam or polyurethane foam cores. The collected data for the micro hardness test is shown in Figure 36 and exhibits comparable hardness across all epoxy samples. As a result there is no additional information that can be extracted to support any possible increased in strength to the epoxy based on the core material.

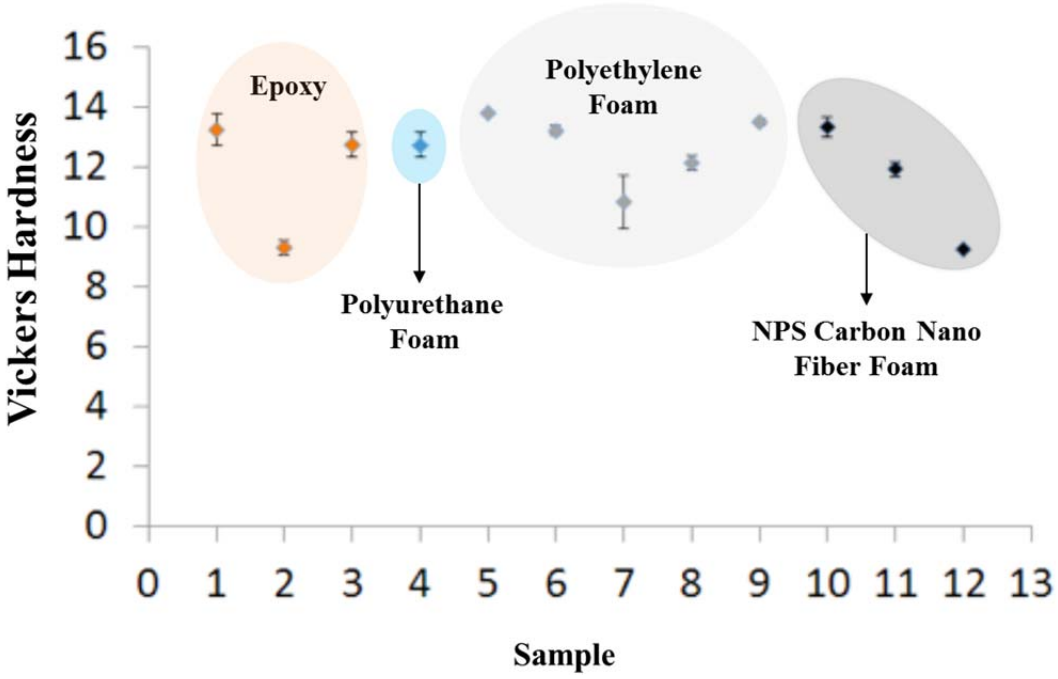

Figure 36. Hardness Testing Results of Epoxy Encased CNFF

Impact testing conducted on the commercial foam samples showed that the carbon nanofiber foam samples had higher impact abortion than the commercial foam samples as shown in Figure 37. The results suggest that the CNFF perform better than commercially available foams and provide evidence of the potential of the CNFF core – epoxy shell structures for energy absorbing applications where low density is required.

CNFF samples had significantly higher impact absorption than commercial foam specimens tested in identical conditions as revealed by the impact test results.

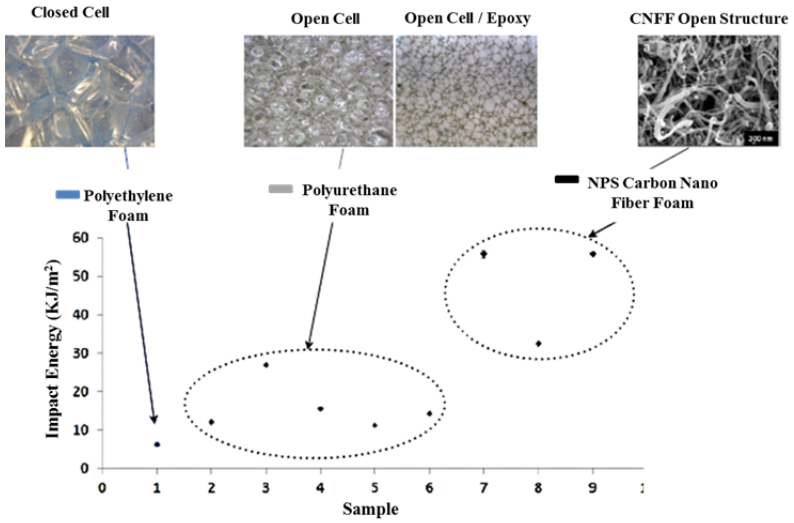

Figure 37. Impact Testing Comparison of Grown Carbon Nanofiber Foam vs. Commercial Foams

The CNFF core-epoxy shell superseded the compressive strength of the epoxy commercial polyethylene and polyurethane foam core- epoxy samples by about 63%, as shown in Figure 38.

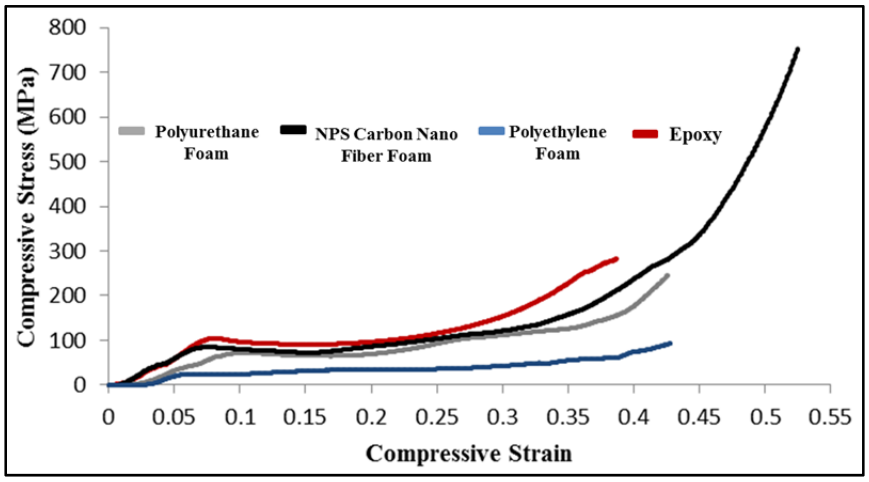

Figure 38. Compression Testing of Carbon Nanofiber Foam vs. Commercial Foams Epoxy Core Shell Until Failure

D. IMPREGNATION OF TUNGSTEN DISULFIDE INTO CARBON NANOFIBER FOAM RESULTS

The scanning electron microcopy images revealed that the impregnation of the inorganic fullerene tungsten disulfide was successful. The SEM images shows the clusters of IF-WS_2 as highlighted in red throughout the CNFF after the impregnating the CNFF with the IF-WS_2 ethanol solution as shown in Figure 39.

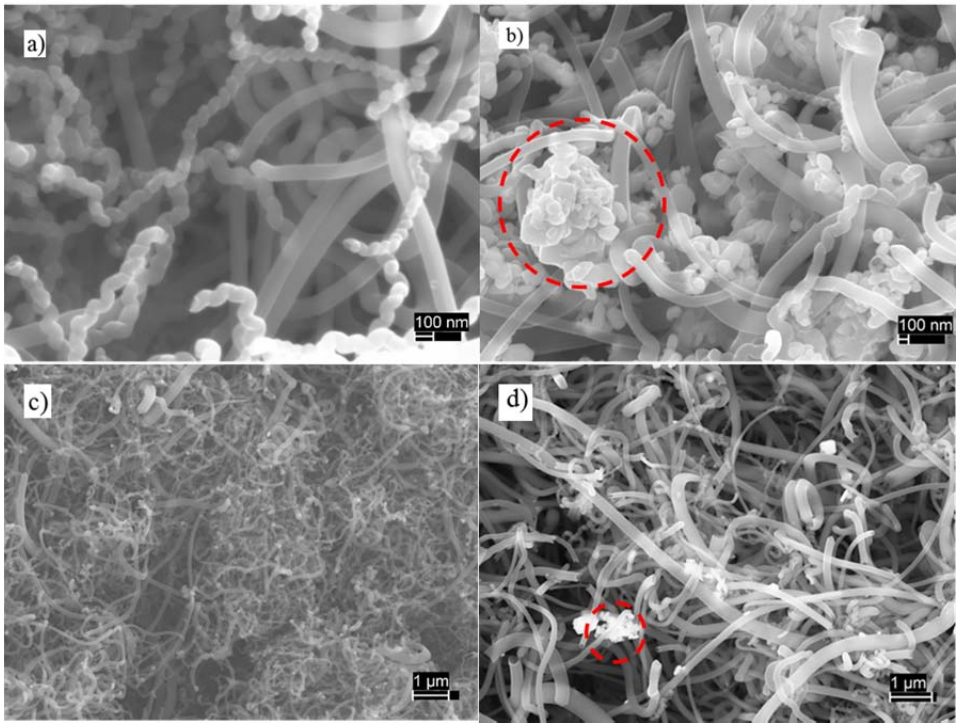

Figure 39. SEM Images of CNFF a) At a 100 nm, b) After 1% IF-WS_2 impregnation at 100 nm, c) At 1µm. d) After 1% IF-WS_2 impregnation at 1µm.

Energy dispersive spectroscopy confirmed the appearance of tungsten (W) and Sulfur (S) as shown in Figure 40. Figure 40a shows the sample prior to impregnating the carbon nanofiber foam with IF-WS_2 and Figure 40b shows the additional detection of the two elements: tungsten label by its element symbol W and sulfur label by its element symbol S.

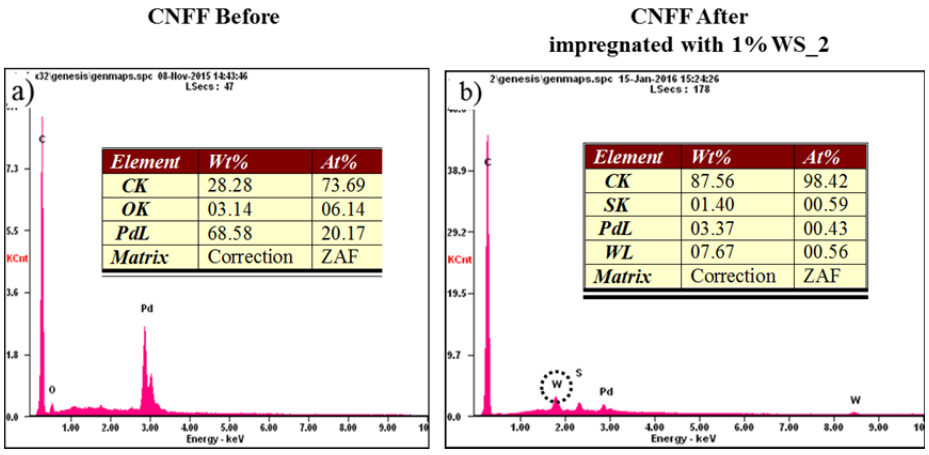

Figure 40. Energy Dispersive Spectroscopy of CNFF Impregnation of IF-WS_2 Results

Element mapping of the carbon nanofiber foam samples impregnated with 1% IF-WS_2 resulted in the validation of the ability to infuse tungsten disulfide into the CNFF uniformly using the impregnation method as shown in Figure 41c identifying the tungsten element in yellow color and Figure 41d identifying the sulfur element in green color. The elemental mapping also identifies carbon as shown in Figure 41a and palladium as shown in dark blue in Figure 41b.

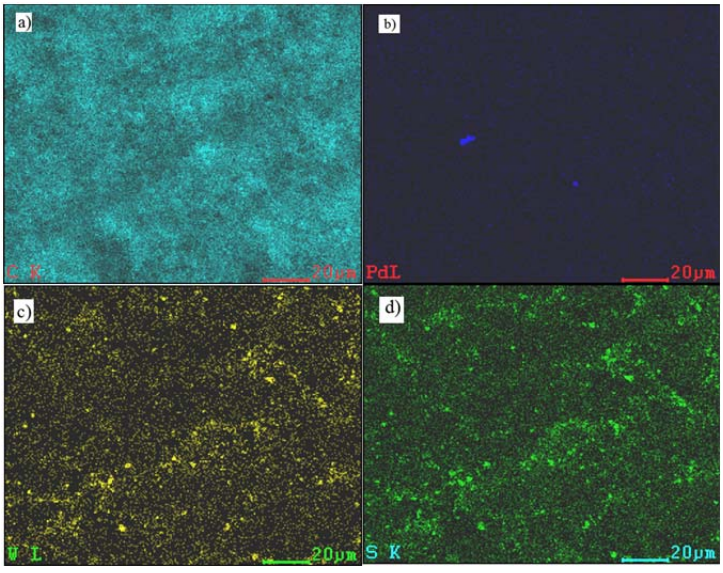

Figure 41. Element Mapping of a) Carbon, b) Palladium, c) Tungsten, and d) Sulfur.

The unconstrained cyclic compression testing results for the carbon nanofiber foam and the CNFF impregnated with 1% WS_2 are shown in Figure 42. The CNFF impregnated with 1% WS_2 has a minimal energy absorption increase of 2.7% in comparison to bare carbon nanofiber foam.

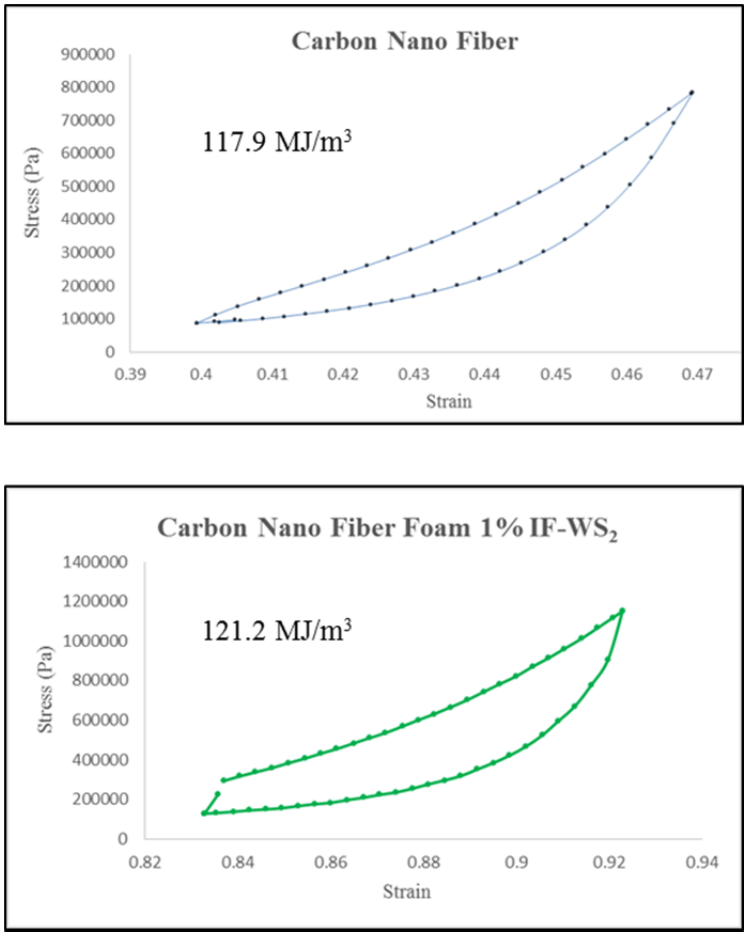

Figure 42. Unconstrained Cyclic Compression Testing of Carbon Nanofiber Foam 1% IF-WS_2 Impregnation.

E. GROWTH OF CARBON NANOFIBER USING A CARBON FRAMEWORK

The CNFF carbon framework hybrids results of using the palladium as a bed are shown in Figure 43. The 10 PPI foam showed the most CNFF growth with a final weight of 1.3329 g. The 20 PPI foam showed less than a 50% CNFF growth coverage with a final weight of .7398 g. The 30 PPI frame had a final weight of .6785 g. The results of the

experiments demonstrate there is a correlation that; as the pores per inch in the foam is increased, the higher the CNFF coverage.

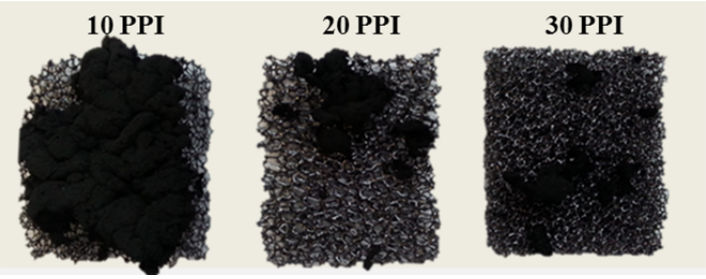

Figure 43. CNFF Growth Over Palladium Bed

More promising results are obtained when the framework was completely submerged into the palladium catalyst suspended methanol mixture and then placed into the mold as shown in Figure 44.

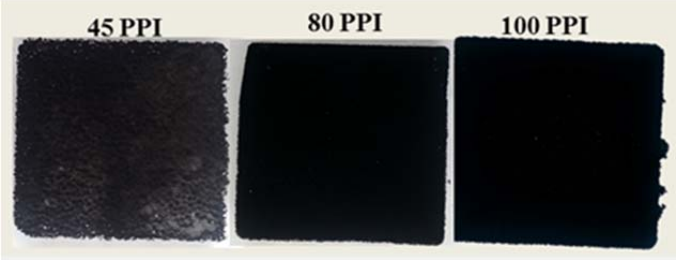

Figure 44. Growth of Carbon Nanofiber Using Wet Impregnation

The growth results are examined using the scanning electron microscopy to obtain images of the carbon commercial frame works as shown in Figure 45. The SEM images collected validate the visual observation described earlier in this section that the escalation in pore per inch leads to an increase in carbon nanofiber growth within the framework as exhibited in Figure 45a the 45 PPI carbon commercial framework has less growth of carbon nanofiber growth compare to Figure 45b SEM image of 80 PPI carbon commercial framework.

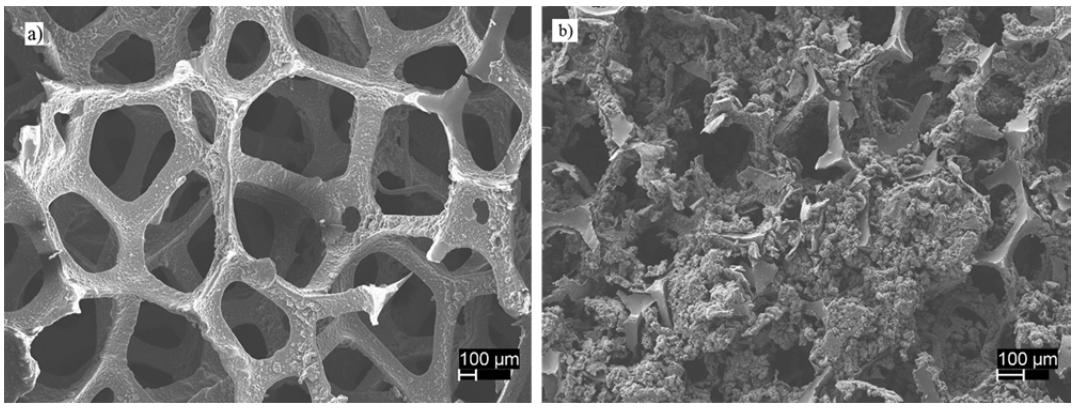

Figure 45. SEM Image of Carbon Commercial Framework Before and After CNFF Growth

The unconstrained compression testing of the carbon frame works a rate of .01 MPa per second from 0 N to failure resulted in the understanding that the growth of the CNFF within the carbon framework did not improve the toughness of the framework. The collected results demonstrate that the carbon frameworks are too brittle and the bare carbon nanofiber foam sample superseded the compressive strength for any of generated carbon frame works structures as shown in Figure 46.

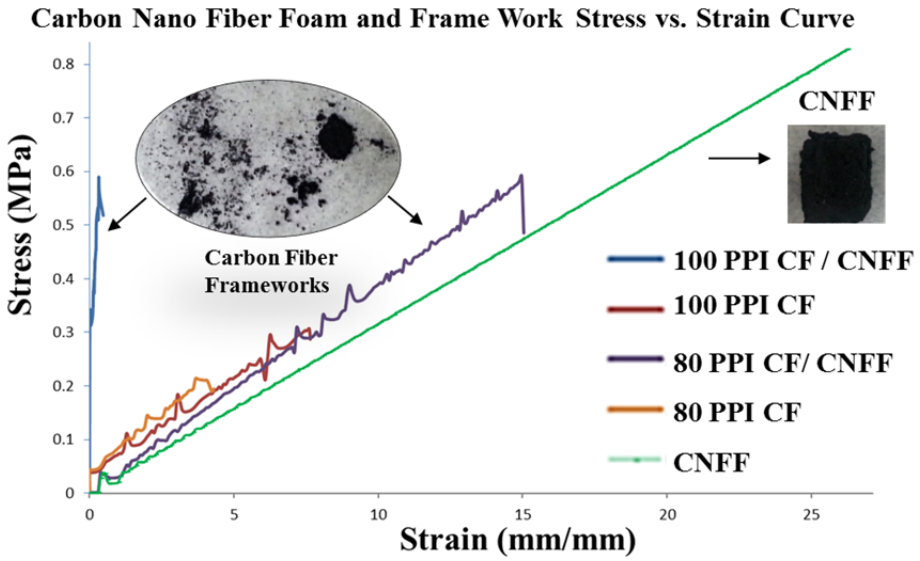

Figure 46. Carbon Nanofiber Foam and Frame Work Stress vs. Strain Curve

F. SHEAR THICKENING FLUIDS / CNFF

1. Shear Thickening Fluids Characterization

Rheological behavior of the shear thickening fluids was determined in at least 3 sample to ensure test repeatability and accuracy. Tests to determine viscosity as a function of strain rate were conducted in ethylene glycol and the diverse mixtures of ethylene glycol with SiO_2 nanoparticles or fumed SiO_2. The three 100% ethylene glycol samples exhibit the same viscosity to shear rate behavior, which validates the shear rheometer results repeatability. The 100% ethylene glycol shows that as the shear rate is increased the viscosity remains approximately constant, as shown in Figure 47. The observed initial peaks from 0 to 100 shear rate is due to the rheometer initial resistance to rotation and dissipates after rotational momentum is achieved.

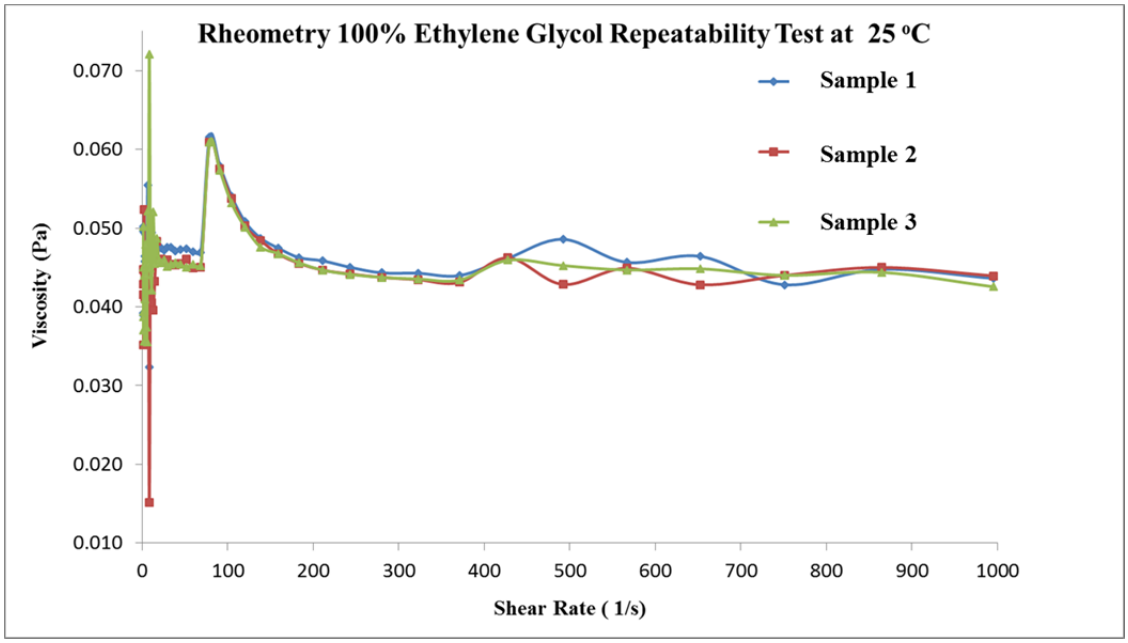

Figure 47. Rheometry 100% Ethylene Glycol Repeatability Test Chart

The results of the silica nanoparticles in ethylene glycol solutions tested with the shear rheometer are shown in Figure 48. The 20% and 30% Silica (SiO_2) nanoparticles rheometer testing resulted in increased in viscosity in comparison to the 100% ethylene glycol but did not exhibit a shear thickening fluid behavior as the viscosity remained

constant as the shear rate increased. In contrast, the 40% Silica (SiO_2) nanoparticles rheometer testing resulted in an steady increase in viscosity up to 1.90 Pa as the shear rate increases up to 400 revolutions per second. The 40% Silica (SiO_2) nanoparticles in ethylene glycol solution proportional increase in viscosity to shear rate revealed the properties desired in a shear thickening fluid.

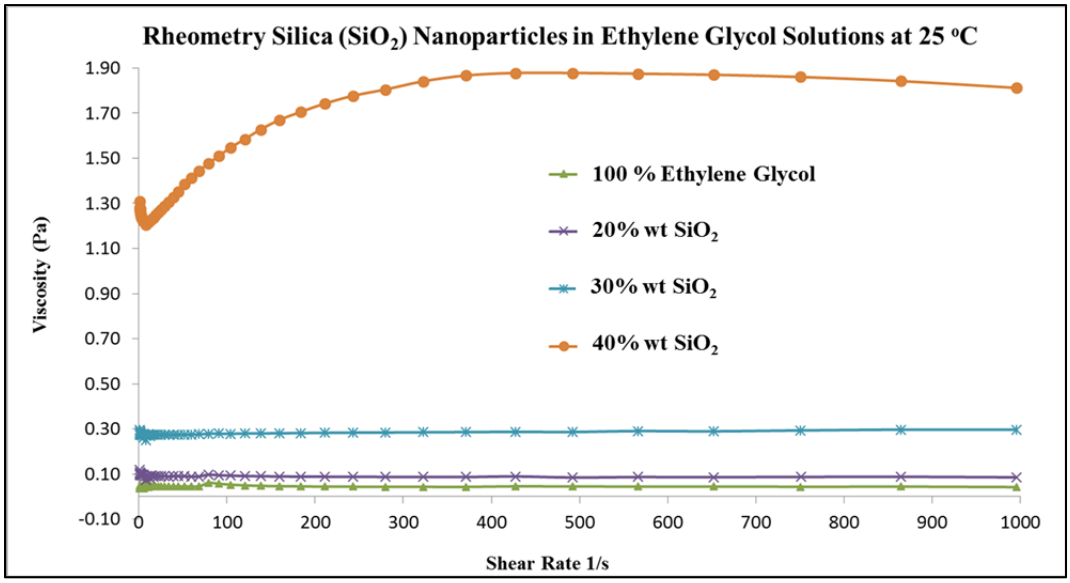

Figure 48. Rheometer Silica (SiO_2) Nanoparticles in Ethylene Glycol Solution Graph

The results of the fumed silica in ethylene glycol solutions tested with the shear rheometer are shown in Figure 49. The fumed silica ethylene glycol solution behaved as a thixotropic substance, that is, as the shear rate increases the viscosity decreases and behaves increasingly as a fluid.

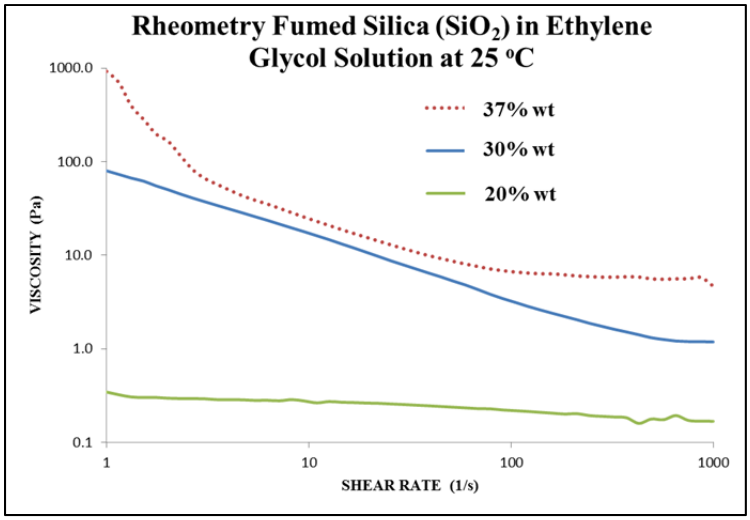

Figure 49. Rheometer Fumed Silica (SiO_2) in Ethylene Glycol Solution Graph

2. Core Epoxy Shell Structures

Only 4 types of samples were the focus of the IZOD impact test; Bare epoxy, CNFF core—Epoxy shell, and 2 CNFF/STF core—epoxy shells. For the later, only the highest percentages of particles (SiO2 nano and fumed SiO2) were used, based on their previously introduced rheological characteristics. Images of cross sectional areas for all the epoxy CNFF combinations are shown in Figure 50.

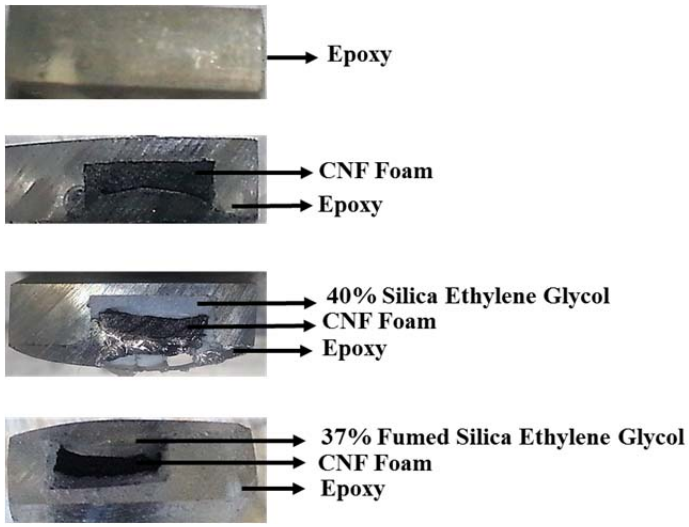

Figure 50. Core Epoxy Shell Structures for IZOD Impact Testing

These core shell structures resulted in a significant improvement of energy absorption when compared to bare epoxy resin. For example, the 40 wt% silica nanoparticle STF and CNFF core—epoxy shell sample outperformed all the other combinations, as shown in Figure 51. The impact testing of the epoxy core shell samples revealed that there was minimal standard deviation between the duplicate samples tested. The combination of CNFF with 40 wt% silica nanoparticle STF encased by an epoxy layer resulted in up to 140% higher break energy (KJ/m^2) when compared to bare epoxy and 33% better when compared to CNFF with epoxy.

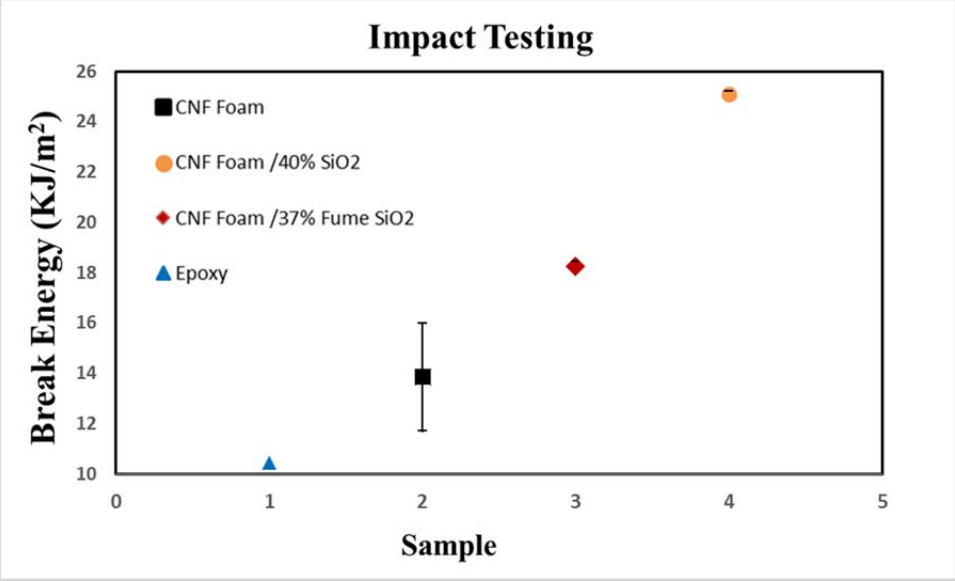

Figure 51. Impact Testing Break Energy per Unit Area Normalized Results for Core Epoxy Shell Structures

Given the interest in developing improved materials that could resist higher impact energies without increasing weight to the wearer, and to simplify the comparison among samples, the results above were normalized by mass. The impact break energy expressed as (KJ/m^2g) for core epoxy shell structures revealed that the break energy of epoxy could be improved by 29% when using CNFF cores, by 57.4% when using CNFF/ fumed silica and up to 101% CNFF/Silica nanoparticles. The break energy for the carbon nanofiber foam with 40 wt% silica nano-particle STF encased by epoxy has the highest energy absorption as shown in Figure 52. The core epoxy shell structure impact testing

findings coincide with the shear thickening fluid rheometer results explained earlier in this chapter.

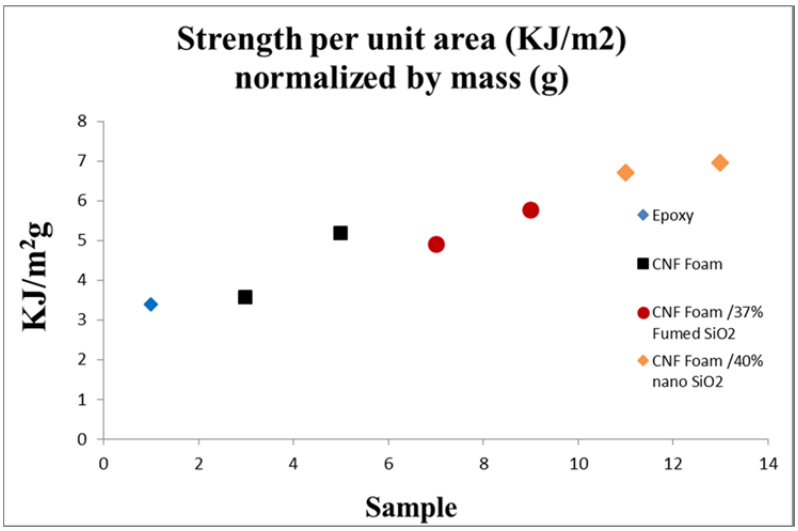

Figure 52. Impact Testing Break Energy per Unit Area Normalized per Mass Results for Core Epoxy Shell Structures

Although shear thickening fluids have been previously used, this manuscript presents the first report of the use of the same with carbon nanofiber foam. All other published data is focused in aramid fibers, which are known to degrade over time or in high light exposure. Indeed, ongoing research is being conducted to develop and fabricate the optimal protective material that can maximize both the shock absorption of a ballistic impact and penetration prevention in combination with minimizing the overall weight of the material. Several research groups concentrate their efforts in strengthening the material currently used in most body armor protection, which is usually made out of Kevlar aramid fiber fabric [29-32].The methods pursued to strengthen the multiple sheet of Kevlar fabric is by either the use of additives such as shear thickening fluids or by the rearrangement of the fibers to maximize the tensile and toughness strength of the fibers. For example, the results in a study done by Young S. Lee et al. in "*The Ballistic Impact characteristics of Kevlar woven fabrics impregnated with a colloidal shear thickening fluid,"* revealed that impregnating Kevlar aramid interwoven fabric with a colloidal shear thickening fluid resulted in an increase in impact resistance without making the material

more rigid. Additionally, the strength gained by the shear thickening fluid allowed for the removal of extra Kevlar sheets which reduced the fabrication costs and weight of the overall material [38]. Research conducted by Tarig A. Hassan et al. in "*Synthesis, processing, characterization of shear thickening fluid (STF) impregnated fabric composites*," a similar experiment was conducted with the use of shear thickening fluid to strengthen Nylon and Kevlar aramid fabrics to test for the effects of sharp objects such as a knife penetration through the fabric as opposed to a ballistic impact. The results of this study revealed that soaking the Nylon and Kevlar fabrics in a shear thickening fluid composed of silica nanoparticles dispersed in liquid polyethylene glycol improve penetration resistance and maintained the flexibility of the material [29, 30]. Thus, we provide herein yet another successful attempt, although using a new base material (CNFF/STF) with the potential to improve performance of personal protective equipment.

In summary, going back to the proposed hypotheses, we found that:

1. Carbon nanofiber foams have higher energy absorption than commercially available foams used for damping applications.
2. The use of carbon and metallic frameworks during the CNFF growth did not strengthen the CNFF and did not increase impact resistance of the foam.
3. The production of carbon nanofiber foam in combination with inorganic fullerene tungsten disulfide, minimally improved the energy absorption properties of the CNFF.
4. The production of carbon nanofiber foam in combination with a shear thickening fluid significantly improved the energy absorption properties of the CNFF.
5. Additionally, the removal of the palladium catalyst from the foam did not significantly alter the mechanical properties of the CNFF.

VI. CONCLUSION

A. OVERVIEW

This work achieved the successful growth of carbon nanofiber foam using the established procedures and the CoFFiN process. The palladium catalyst extraction treatment used on the carbon nanofiber foam confirmed to be a valid process that would reduce the fibers growth expenses while maintaining the mechanical properties of the foam.

The mechanical properties of carbon nanofiber foam in comparison with commercially foams used for vibration dampening were tested and demonstrated that the carbon nanofiber foam absorbs 95.6% more energy compared to the polyurethane commercial foam and 77.3% more energy compared with the polyethylene commercial foam.

The impregnation of IF-WS2 into the carbon nanofiber foam was successfully achieved. However, it obtained minimal energy absorption, with an increase of only 2.7% in comparison to bare carbon nanofiber foam.

The growth of carbon nanofibers foam using carbon frameworks did not enhance the energy absorption properties of the original CNFF. Combining the CNFF with the frameworks resulted in very brittle materials that lacked the viscoelastic behavior necessary for energy absorption applications. However, the carbon frameworks gained some toughness with the growth of carbon nanofibers foam within the framework. These finding might have other applications that require a very light material that can withstand sustained higher temperatures where high impact resistance is not necessary for their use.

The colloidal suspension that behaved as a shear thickening fluid of the silica nanoparticles was effectively produced. Dissimilarly the fumed silica powder in ethylene glycol behaved as a thixotropic liquid which could serve well as a lubricant.

This research validated that shear thickening fluid was successfully introduced into carbon nanofiber foam to improve the energy absorption properties of the CNFF generated structure. The combination of carbon nanofiber foam and shear thickening

fluid encased by an epoxy layer resulted in core-shell structures with significant improvements in energy resistance, up to 140% higher when compared to bare epoxy and 33% better when compared to carbon nanofiber foam and epoxy. The results of this work produced an energy absorbent new base material (CNFF/STF) with potential to improve performance of personal protective equipment.

B. PUBLICATIONS

The results of this work led to the production of two articles:

1. *"Scaling up the Fabrication of Mechanical- Robust Carbon Nanofiber Foams."* Published on 15 February 2016. This article includes the mechanical testing of the carbon nanofiber foam, the catalyst removal process and mechanical analysis [15].

2. The second article will include the shear thickening fluid development, characterization, and mechanical testing in combination with the carbon nanofiber foam multifunctional structures.

C. RECOMMENDATIONS FOR FUTURE RESEARCH

Prospective work should be directed to examine the environmental effects and hazards of the carbon nanofiber foam. Further research on the shear rate increase behavior of fullerene tungsten disulfide in a suspension should be conducted for lubricant applications.

LIST OF REFERENCES

[1] C. Dean, “The modern warriors combat load: dismounted operations in Afghanistan April-May 2003,” *U. S. Army Center for Army Lessons Learned,* pp. 1–119, May 2003.

[2] A. K. Bandaru, V. V. Chavan, S. Ahmad, R. Alagirusamy and N. Bhatnagar, “Ballistic impact response of Kevlar (R) reinforced thermoplastic composite armors,” *Int. J. Impact Eng.,* vol. 89, pp. 1–13, Mar. 2016.

[3] S. Chocron, N. King, R. Bigger, J. D. Walker, U. Heisserer and H. van der Werff, “Impacts and waves in Dyneema (R) HB80 strips and laminates,” *Journal of Applied Mechanics-Transactions of the ASME,* vol. 80, pp. 031806, May 2013.

[4] E. S. Greenhalgh, V. M. Bloodworth, L. Iannucci and D. Pope, “Fractographic observations on Dyneema (R) composites under ballistic impact,” *Composites Part A-Applied Science and Manufacturing,* vol. 44, pp. 51–62, Jan. 2013.

[5] P. J. Hazell, G. J. Appleby-Thomas, X. Trinquant and D. J. Chapman, “In-fiber shock propagation in Dyneema (R),” *J. Appl. Phys.,* vol. 110, pp. 043504, Aug. 15, 2011.

[6] M. Hudspeth, X. Nie and W. Chen, “Dynamic failure of Dyneema SK76 single fibers under biaxial shear/tension,” *Polymer,* vol. 53, pp. 5568–5574, Nov. 9, 2012.

[7] S. N. Monteiro, E. P. Lima Jr., L. H. L. Louro, L. C. Da Silva and J. W. Drelich, “Unlocking function of aramid fibers in multilayered ballistic armor,” *Metallurgical and Materials Transactions A-Physical Metallurgy and Materials Science,* vol. 46A, pp. 37–40, Jan. 2015.

[8] R. Odonnell, “Deformation energy of Kevlar backing plates for ceramic armors,” *J. Mater. Sci. Lett.,* vol. 12, pp. 1485–1486, Sep. 15, 1993.

[9] Z. Zhang, S. Shen, H. Song and D. Zhang, “Ballistic penetration of Dyneema fiber laminate,” *Journal of Materials Science & Technology,* vol. 14, pp. 265–268, May 1998.

[10] V. S. Berg, D. S. Preece, J. H. Stofleth and M. A. Risenmay, *Kevlar and Carbon Composite Body Armor—Analysis and Testing.* 2005.

[11] M. A. Atwater, J. Phillips and Z. C. Leseman, “Formation of carbon nanofibers and thin films catalyzed by palladium in ethylene-hydrogen mixtures,” *Journal of Physical Chemistry C,* vol. 114, pp. 393–397, Apr. 8, 2010.

[12] M. A. Atwater, A. K. Mousavi, Z. C. Leseman and J. Phillips, “Density carbon fiber foam and its characterization a strain gauge,” *Carbon,* vol. 57, pp. 363–370, June 2013.

[13] M. A. Atwater, A. K. Mousavi, Z. C. Leseman and J. Phillips, “Direct synthesis and characterization of a nanowoven structure comprised of carbon nanofibers,” *Pergamon,* vol. 57, pp. 363–370, June 2013.

[14] W. Curtin, P. Arias Monje, C. Dominguez, J. Phillips and C. Luhrs C, “Scaling up the fabrication of mechanical robust carbon nanofibers foams,” *Fibers,* 2015.

[15] W. Curtin J., “Fabrication of a mechanically robust carbon nanofiber foam,” *M. S. Thesis,* June 2016.

[16] C. Luhrs C., C. Daskam, E. Gonzalez and J. Phillips, “Fabrication of a low density carbon fiber foam and its characterization a strain gauge,” *Materials,* vol. 7, pp. 3699–3714, 2014.

[17] M. A. Atwater, J. Phillips, S. K. Doorn, C. Luhrs C., Y. Fernandez, J. A. Menendez and Z. C. Leseman, “The production of carbon nano fibes and thin films on palladium catalysts from ethylene-oxygen mixtures.” *Carbon,* vol. 47, pp. 2269–2280, 2009.

[18] R. T. Baker K., M. Barber A., R. Waite J., P. Harris S. and F. Feates S., “Nucleation and Growth of Carbon Deposits from Nickel Catalyzed Decomposition of Acetylene,” *Journal of Catalysis,* vol. 26, pp. 51-&, 1972.

[19] C. Daskam, “Mechanical and electrical characterization of novel carbon nanofiber ultralow density Foam,” *M. S. Thesis, NPS, Monterey, California,* December 2013.

[20] S. Kaur, P. M. Ajayan and R. S. Kane, “Design and characterization of three-dimensional carbon nanotube foams.” *J. Phys. Chem, B,* vol. 110, pp. 21377-21380, 2006.

[21] M. Kumar and Y. Ando, “Chemical vapor deposition of carbon nanotubes: a review on growth mechanism and mass production,” *Journal Nano Science and Nanotechnology,* vol. 10, pp. 3739–3758, Jan 2010.

[22] K. Kolasinski, “Catalytic growth of nanowires: vapor–liquid–solid, vapor–solid–solid, solution–liquid–solid and solid–liquid–solid growth,” *Current Opinion in Solid State and Materials Science,* vol. 10, pp. 182–191, Jun. 2006.

[23] J. Phillips, T. Shiina, M. Nemer and K. Lester, “Graphitic structures by design,” *Lanmuir,* vol. 22, pp. 9694–9703, Nov. 7, 2006.

[24] Zhu, Yan. Qiu, et al., “WS_2 and MoS_2 inorganic fullerenes-super shock absorbers at very high pressures,” *Advanced Materials,* vol. 17, pp. 1500–1503, 2005.

[25] J. Cook, S. Rhyans, L. Roncase, G. Hobson and C. Luhrs C., "Microstructural study of IF-WS_2 failure mode," *Inorganics,* vol. 2, pp. 377–395, 2014.

[26] L. Margulis, R. Tenne and S. Iijima, "Nucleation of WS_2 fullerenes at room temperature." *Microsc. Microanal. Microstruc.t,* vol. 7, pp. 87–89, 1996.

[27] R. Tenne, L. Margulis, M. Genut and G. Hodes, "Polyhedral and cylindrical structures of tungsten disulfide," *Nature,* vol. 360, pp. 444–446, 1992.

[28] *Doucel Reticulated Vitreous Carbon Foam (RVC) Product Specification.* Available: http://www.ergaerospace.com/RVC-properties.html. June 3, 2016.

[29] T. A. Hassan, V. K. Rangari and S. Jeelani, "Synthesis, processing, characterization of shear thickening fluid (STF) impregnated fabric composites." *Material Science and Engineering A.,* vol. 527, pp. 2892–2899, January 6, 2010.

[30] T. A. Hassan, V. K. Rangari and S. Jeelani, "Sonochemical synthesis and rheological properties of shear thickening silica dispersions," *Ultrasonics Sonochemistry,* pp. 947–952, February 08, 2010.

[31] M. J. Decker, C. J. Halbach, C. H. Nam, N. J. Wagner and E. D. Wetzel, "Stab resistance of shear thickening fluid (STF) -treated fabrics," *Composites Science and Technology,* vol. 67, pp. 565–578, August 3, 2006.

[32] X. Zhang, W. Li and X. Gong, "Study on magnetorheological shear thickening fluid," *Smart Materials and Structures,* vol. 17, pp. 6, January 17, 2008.

[33] *Eggcrate charcoal regular foam*. Available: http://www.foambymail.com/EC/eggcrate-charcoal-regular-foam.html. DOI: May 27, 2016.

[34] *Polyethylene foam sheets- 1.7 LB blue*. Available: http://www.foambymail.com/PE17-_2/polyethylene-foam-sheets-1-7lb-blue.html. DOI: May 27, 2016.

[35] A. Reyes, *Beginner's guide to SolidWorks 2013—Level I Parts, Assemblies, Drawings, Simulation Xpress.* Schroff Development Corp. Publications, 2013.

[36] M. Dunlap and J. Dr. Adaskaveg E, "Introduction to the scanning electron microscope," 1997.

[37] W. S. Rasband, "Image J," *National Institutes of Health, Bethesda, Maryland, USA,* 1997–2012.

[38] Y. Lee, E. D. Wetzel and N. J. Wagner, "The ballistic impact characteristics of Kevlar woven fabrics impregnated with a colloidal shear thickening fluid," *Journal of Material Science,* vol. 38, pp. 2825–2833, 2003.

THIS PAGE INTENTIONALLY LEFT BLANK

INITIAL DISTRIBUTION LIST

1. Defense Technical Information Center
   Ft. Belvoir, Virginia

2. Dudley Knox Library
   Naval Postgraduate School
   Monterey, California